We are IntechOpen, the world's leading publisher of Open Access books Built by scientists, for scientists

4,800
Open access books available

122,000
International authors and editors

135M
Downloads

Our authors are among the

154
Countries delivered to

TOP 1%
most cited scientists

12.2%
Contributors from top 500 universities

CLARIVATE ANALYTICS BOOK CITATION INDEX INDEXED

WEB OF SCIENCE™

Selection of our books indexed in the Book Citation Index in Web of Science™ Core Collection (BKCI)

Interested in publishing with us?
Contact book.department@intechopen.com

Numbers displayed above are based on latest data collected.
For more information visit www.intechopen.com

16

Nanocomposite and Nanostructured Carbon-based Films as Growth Substrates for Bone Cells

Lucie Bacakova[1], Lubica Grausova[1], Jiri Vacik[2], Alexander Kromka[3], Hynek Biederman[4], Andrei Choukourov[4] and Vladimir Stary[5]

[1]*Department of Growth and Differentiation of Cell Populations, Institute of Physiology, Academy of Sciences of the Czech Republic, Prague,*
[2]*Nuclear Physics Institute, Academy of Sciences of the Czech Republic & Research Center Rez,*
[3]*Institute of Physics, Academy of Sciences of the Czech Republic, Prague,*
[4]*Department of Macromolecular Physics, Faculty of Mathematics and Physics, Charles University, Prague,*
[5]*Faculty of Mechanical Engineering, Czech Technical University, Prague, Czech Republic*

1. Introduction

In recent years, the need to substitute and repair damaged hard tissues (bone, joints, teeth) has been increasing due to diseases and injuries of the locomotory system, which are relatively widespread in the civilized world. The most frequently used implants are based on metals; for example, the metallic part of the socket and the metallic stem of a total hip prosthesis, anchored to the hip-bone and femur, respectively, or dental implants anchored to the jawbone. In bone implants, primary stability is determined mainly by the shape of the implant and by the quality of the bone preparation. However, the secondary stability depends strongly on the attractiveness of the implant surface for the adhesion, growth and phenotypic maturation of osteoblasts, and the formation of mineralized bone tissue at the bone-implant interface. The attractiveness of an implant for colonization with bone cells can be markedly enhanced by various surface modifications of the implant, e.g., by deposition of nanocomposite and nanostructured films.

In this chapter, we summarize more than ten years of experience in our laboratory (in the context of investigations by other authors) of studying the interaction of bone cells *in vitro* with various types of nanocomposite layers based on carbon and carbon enriched with metalloid or metal atoms. These layers include nanocomposite hydrocarbon plasma polymer (ppCH) films with various concentrations of Ti or Ag, titanium-enriched amorphous carbon (C:Ti), pyrolytic graphite and also novel boron-doped nanocrystalline diamond films, nanostructured hybrid fullerene C_{60}/Ti composite films and carbon nanotube-based substrates.

The nanocomposite films are expected to support their colonization with cells particularly by their nanoscale surface roughness, i.e., the presence of irregularities smaller than 100 nm.

The surface nano-roughness mimics, at least to some degree, the nanoarchitecture of the natural extracellular matrix (ECM) as well as of the cell membrane, such as the size of some ECM molecules, their folding and branching, or prominences on the cell membrane, e.g., extracellular parts of the cell adhesion receptors. The nanostructure of a material also improves the adsorption of cell adhesion-mediating ECM molecules, present in biological fluids, such as the serum supplement of cell culture media, blood or interstitial fluid, or synthesized and deposited by cells contacting the material. These molecules involve, e.g., vitronectin, fibronectin, collagen, laminin and also fibrin, a molecule of the provisional matrix formed during tissue healing. On nanostructured materials, the cell adhesion-mediating molecules are adsorbed in advantageous geometrical conformations, allowing for good accessibility of the active sites in these molecules by the cell adhesion receptors (Webster *et al.,* 2000; Price *et al.,* 2004). The active sites include specific amino acid sequences, e.g., Arg-Gly-Asp (RGD), bound by many cells types, or cell-specific sequences, such as Lys-Arg-Ser-Arg (KRSR), Arg-Glu-Asp-Val (REDV) and Val-Ala-Pro-Gly (VAPG), bound by osteoblasts, vascular endothelial cells and vascular smooth muscle cells, respectively. The cells bind the active sites in the matrix molecules by their cell adhesion receptors. The most known and systemized are receptors of the integrin superfamily, but non-integrin receptors, usually of the proteoglycan nature, also take an important place in the cell adhesion. The non-integrin receptors can bind either specific amino acid sequences, e.g., VAPG, or other specific saccharide ligands also present in the cell adhesion-mediating ECM molecules (for a review, see Bacakova *et al.,* 2004; 2008a; Bacakova and Svorcik 2008).

In addition, nanostructured surfaces are believed to preferentially adsorb vitronectin, due to its relatively small and linear molecule compared to the larger and more complicated, e.g., branched, molecules of other ECM proteins (Webster *et al.,* 2000; Price *et al.,* 2004). Vitronectin is then preferentially recognized by osteoblasts rather than by other cell types, thus nanostructured surfaces are considered to be particularly suitable for bone tissue engineering.

In supporting the protein adsorption and cell adhesion, the nanoscale-roughness acts synergistically with the polarity and wettability of the material surface, which is often due to the presence of oxygen-containing chemical functional groups on the surface. On wettable surfaces, the cell adhesion-mediating molecules are adsorbed in a flexible and reorganisable form, enabling good accessibility of specific sites on these molecules by the cell adhesion receptors. In our earlier studies on ion-irradiated polymers, the creation of oxygen-containing groups on the polymer surface and the increased material wettability were associated with increased adsorption of collagen IV and enhanced adhesion, growth and phenotypic maturation of vascular endothelial and smooth muscle cells in cultures on the polymers (Bacakova *et al.,* 2000, 2001a). In comparison with hydrophobic surfaces, the wettable surfaces also adsorb a lower amount of albumin, i.e., a protein non-adhesive for cells. However, the cell adhesion is optimal only on moderately wettable surfaces. On highly hydrophilic surfaces, e.g., on oxygen-terminated nanocrystalline diamond (water drop contact angle less than 2°; Clem *et al.,* 2008) or surfaces with PEO chains, particularly in the form of brush, mobile in water environment (Bacakova *et al.,* 2007a), the cell adhesion-mediating molecules were not adsorbed at all or very weakly, which disabled or significantly limited the cell adhesion.

Another important property of some carbon-based materials, particularly nanocrystalline diamond films doped with boron or substrates with carbon nanotubes, is the electroactivity of these substrates, e.g., their electrical charge, electrical potential and electrical conductivity, which enable the electrical stimulation of cells (Supronowicz *et al.,* 2002;

Kromka *et al.,* 2010). Interestingly, the adhesion, growth, maturation and function of cells on electroactive surfaces are improved even without active stimulation of cells with an electrical current. The underlying mechanism probably includes enhanced adsorption of cell adhesion-mediating proteins, a more advantageous geometrical conformation of these proteins for their accessibility by cell adhesion receptors and facilitation of cellular processes, such as activation of ion channels in the cell membrane, movement of charged molecules inside and outside the cell, upregulated mitochondrial activity and enhanced proteosynthesis (for a review, see Schmidt *et al.,* 1997; Gomez and Schmidt, 2007; Khang *et al.,* 2008; Shi *et al.,* 2008).

Last but not least, the nanocomposite films can significantly increase the mechanical and chemical resistance of the implant surface. In other words, these coatings can prevent the release of ions and material particles from the bulk material. For example, NCD films impermeably covered the underlying silicon substrates, which in their uncoated state acted as highly cytotoxic for cells, and carbon-titanium layers deposited on carbon fiber-reinforced carbon composites significantly attenuated the release of carbon particles from these materials.

Thus, all nanocomposite layers mentioned in this chapter are promising for coating biomaterials designed for hard tissue implantation in order to enhance their integration with the surrounding tissue. The potential use of our nanocomposite films for constructing biosensors and biostimulators (boron-doped NCD films) or micropatterned surfaces for regionally-selective cell adhesion and directed cell growth (fullerene C_{60}/Ti composite films) are other promising applications, which are discussed in this chapter.

2. Hydrocarbon plasma polymers

Plasma polymers (Tab. 1) are materials created from small organic molecules (e.g., methane, n-hexane, acrylic acid, octadiene, tetrafluoroethylene, acetonitrile) by glow discharge, which is usually carried out at low temperatures, low pressures and without solvents. Glow discharge as a source of highly energetic electrons and UV radiation causes ionization, excitation and fragmentation of the monomer molecules employed, creating a number of reactive chemical species, which further participate in crosslinking and formation of quazi-polymeric network. Thus, plasma polymers differ from conventional polymers, i.e., materials with chains containing regularly repeated monomer units, by short and randomly branched chains. Plasma polymers usually exist in the form of thin films which can be deposited on various substrates, such as glass, metals, silicon, polystyrene cell culture dishes etc. These films have a broad spectrum of applications, including use in medicine and various biotechnologies (for a review, see Biederman 2004). For example, plasma polymers have been used for the creation of antibacterial coatings of body implants and other medical devices (Vasilev *et al.,* 2010), surfaces for studying protein adsorption (Zhang and Feng 2007), protein interaction (Menzies *et al.,* 2010), protein separation (Tsai *et al.,* 2003), and also for immobilization of proteins (Kim *et al.,* 2003), e.g., enzymes, such as lysozyme (Thierry *et al.,* 2008) or trypsin (Abbas *et al.,* 2009). Plasma polymer films with immobilized heparin can serve as hemocompatible surfaces preventing blood coagulation (Yang *et al.,* 2010). Another broad and advanced application of plasma polymers is the construction of biosensors (Seyama *et al.,* 2004; Chu *et al.,* 2009).

As for interaction with anchorage-dependent cells, plasma polymer films can be constructed as repulsive or attractive for cells. For example, a plasma polymer of methane was

constructed to prevent cell and tissue adhesion on contact lenses (Ho and Yasuda 1988), while plasma polymers of acrylic acid supported the adhesion of epithelial cells on special therapeutic contact lenses designed to transfer these cells onto the denuded rabbit cornea *in vitro* (Deshpande *et al.,* 2009). Acrylic acid-based surfaces were used for the creation of cell sheets for tissue engineering (Majani *et al.,* 2010). Cell-attractive and cell-repulsive plasma polymers have also been combined in order to create micropatterned surfaces for regionally-selective adhesion and directed growth of cells. For example, surfaces containing cell-adhesive microdomains of tetrafluoroethylene, placed on a cell-repulsive background of tetraethylene glycol dimethyl ether, were used for controlling the shape, degree of spreading, assembly of actin cytoskeleton, phenotypic modulation and proliferation of vascular smooth muscle cells (Goessl *et al.,* 2001). Similarly, cell-repellent domains of poly(ethylene) oxide-like plasma-deposited films, combined with cell-adhesive poly-L-lysine domains, were used for controlled adhesion, arrangement and neurite outgrowth of human neural stem cells derived from umbilical cord blood (Ruiz *et al.,* 2008). In our earlier study (Filova *et al.,* 2009), micropatterned surfaces were prepared by the successive plasma polymerization of acrylic acid (AA) and 1,7-octadiene (OD) through a metallic mask on the inner surface of 24-well polystyrene multidishes. A reactor with a cooper radio frequency power source for initiating and sustaining the plasma was used for this procedure. Rat vascular smooth muscle cells (VSMC), bovine endothelial cells (EC), porcine mesenchymal stem cells (MSC) or human skeletal muscle cells (HSKMC) seeded on these surfaces adhered and grew preferentially on hydrophilic strip-like AA domains rather than on hydrophobic OD domains. In addition, both VSMC and EC on AA domains displayed a higher degree of phenotypic maturation. In VSMC, this was manifested by a higher concentration of alpha-actin (i.e., an important marker of VSMC differentiation towards the contractile phenotype), measured per mg of protein in cell homogenates by an enzyme-linked immunosorbent assay. In EC on AA domains, immunofluorescence staining showed more apparent Weibel-Palade bodies, containing the von Willebrand factor. Also MSC growing on AA domains had a better developed beta-actin cytoskeleton, and also contained a higher concentration of beta-actin per mg of protein (Filova *et al.,* 2009).

Our other earlier studies were focused on composites of hydrocarbon plasma polymers with metals, namely titanium or silver (Bacakova *et al.,* 2008b; Grinevich *et al.,* 2009). The benefits of composite materials arise from combining materials with very different properties to produce structural or functional properties not present in any individual component. The type and concentration of the metal component in the hydrocarbon plasma polymers, such as silver, molybdenum, nickel, germanium or titanium, significantly influence the optical, electrical and mechanical properties of these composites. Metal/hard carbon plasma polymer thin films have been a special issue among the carbon-based materials, because of their favorable properties such as high hardness, low friction coefficient, high wear resistance, optical transparency and chemical inertness. The advantageous physicochemical properties of these films are important not only for their industrial applications but also for their use in medicine and in various biotechnologies.

In our earlier study (Grinevich *et al.,* 2009), nanocomposite Ti/hydrocarbon plasma polymer (Ti/ppCH) films were deposited by DC magnetron sputtering of a titanium target in n-hexane, argon or a mixture of these two gases. The resultant films were heterogeneous with inorganic regions of nanometer scale distributed within a plasma polymer matrix. The titanium content was controlled by adjusting the argon/n-hexane ratio in the working gas. In the pure n-hexane atmosphere, the Ti concentration was found to be below 1 atomic %,

whereas in pure argon, it reached 20 atomic %, as revealed by Rutherford Backscattering/Elastic Recoil Detection Analysis (RBS/ERDA). A high level of titanium oxidation was detected with TiO_2, sub-stoichiometric titania and titanium carbide composing an inorganic phase of the composite films. In addition, high hydrogen content was detected in films rich with titanium.

As for the interaction with cells, Ti-deficient and Ti-rich films proved to be equally good substrates for adhesion and growth of cultured human osteoblast-like MG 63 cells. In these cells, the population densities on days 1, 3 and 7 after seeding, spreading area on day 1, formation of talin-containing focal adhesion plaques, as well as concentrations of talin and osteocalcin (per mg of protein), were comparable to the parameters obtained in cells on the reference cell culture materials, represented by microscopic glass coverslips or polystyrene dishes. In contrast to our results, the number of rat bone marrow cells in primary or low-passaged cultures on a similar material, i.e., amorphous hydrogenated carbon with 0 to 13 atomic % of Ti, was significantly increased on Ti-containing samples compared to cells on glass (Schroeder *et al.,* 2000). In addition, the activity of alkaline phosphatase, an important marker of osteoblastic cell differentiation, tended to be higher in the cells on films with higher Ti concentrations. This disproportion between our results and results of the study by Schroeder *et al.,* (2000) may be explained by a higher sensitivity of primocultured or low-passaged bone marrow cells to physical and chemical properties of the material surface in comparison with the line MG 63 used in our study, which is tumor-derived, highly passaged and well-adapted to long-term cultivation *in vitro* conditions. Similar higher sensitivity to the roughness, topography and other physical and chemical surface properties were observed in our earlier study in rat vascular smooth muscle cells (VSMC) in low-passaged cultures on carbon fiber-reinforced carbon composites (CFRC) coated by a carbon-titanium layer. The increase in cell adhesion and growth on Ti-containing surfaces was more pronounced in VSMC than in MG 63 cells (Bacakova *et al.,* 2001b).

However, another cell line, namely bovine pulmonary artery endothelial CPAE cells, reacted sensitively to the presence of Ti in the ppCH films. The cell population densities, cell spreading area and also the concentration of von Willebrand factor, a marker of endothelial cell maturation, were significantly higher in CPAE cells on Ti-rich than on Ti-deficient films. On Ti-rich films, these parameters were also higher or similar in comparison with the reference cell culture materials. The main underlying mechanism of this cell response is probably an increased content of oxygen in the Ti-rich films, which is present in the form of TiO, TiO_2 and oxygen-containing chemical functional groups, such as C-O, C=O and O-C=O. The increased oxygen content leads to a higher wettability of the material surface and improved adsorption of cell adhesion-mediating molecules in a flexible form, enabling good accessibility of specific sites on these molecules by cell adhesion receptor (Bacakova *et al.,* 2000, 2001a; for a review, see Bacakova and Svorcik 2008).

Another important factor improving the protein adsorption and cell adhesion is the nanoscale roughness of the material surface, which resembles the nanoarchitecture of the natural extracellular matrix (ECM). However, both Ti-deficient and Ti-rich films in our study (Grinevich *et al.,* 2009) were of similar nano-roughness (root mean square roughness, RMS, was in the range of 1-6 nm), as measured by Atomic Force Microscopy (AFM) on the 1x1 μm images.

Thus, both Ti-deficient and Ti-rich hydrocarbon plasma polymer films could be used for coating bone implants, the Ti-rich film also being effective in enhancing the endothelialization of blood contacting artificial materials (Grinevich *et al.,* 2009).

Table 1. Classification of carbon films by Fraunhofer Institute, © 2009. Electronic Name Index of Carbon Coatings at http://www.ist.fraunhofer.de/english/c-products/tab/complete.html

	Carbon films									
Designation	**1 Plasma-polymer films**	**2 Amorphous carbon films (diamond-like-carbon films / DLC)**								
Thin film / thick film	Thin film	Thin film							Th	
Doping, additional elements		hydrogen-free			hydrogenated				undope	
				modified			modified			
				with metal			with metal	with non-metal		
Crystal size on the growth side	./.	(amorphous)							1 to 500 nm, nano-crystalline	0. 10 m cr
Predominating C-C-bond type	sp^2 or sp^3, linear bond	sp^2	sp^3	sp^2	sp^2 or sp^3	sp^3	sp^2	sp^2	sp^3	sp
Film No.	**1**	**2.1**	**2.2**	**2.3**	**2.4**	**2.5**	**2.6**	**2.7**	**3.1**	**3.**
Designation	**Plasma-polymer film**	**Hydrogen-free amorphous carbon film**	**Tetrahedral hydrogen-free amorphous carbon film**	**Metal-containing hydrogen-free amorphous carbon film**	**Hydrogenated amorphous carbon film**	**Tetrahedral hydrogenated amorphous carbon film**	**Metal-containing hydrogenated amorphous carbon film**	**Modified hydrogenated amorphous carbon film**	**nano-crystalline CVD diamond film**	**m cr C di fil**
Recommended abbreviation	./.	a-C	ta-C	a-C:Me	a-C:H	ta-C:H	a-C:H:Me (Me = W, Ti, ...)	a-C:H:X (X = Si, O, N, F, B, ...)	./.	

Hydrocarbon plasma polymers (Bacakova *et al.,* 2008b) or amine plasma polymers (Vasilev *et al.,* 2010) have also been combined with silver in order to create antimicrobial surfaces. Silver atoms can bind bacterial DNA, inactivate bacterial proteins, inhibit a number of important transport processes of bacterial cells and interact with cellular oxidation processes, as well as the respiratory chain. Silver has been used as an important component of bioactive wound dressings, eye drops, urinary, vascular and blood dialysis catheters, artificial vascular grafts and heart valves, devices for bone fixation, orthopaedic and dental implants, bone cements, three-dimensional scaffolds designed for engineering various tissues, e.g., bone, and sponges for the potential construction of bioartificial skin (for a review, see Bacakova *et al.,* 2008b, Vasilev *et al.,* 2010). In comparison with synthetic antibiotics, the advantage of silver is to kill a much wider spectrum of microbes and not to develop resistance. However, the disadvantage is cytotoxicity of silver for mammalian cells, which is based on the inhibitory action of silver on DNA synthesis, damage and loss of cellular proteins, mitochondrial dysfunction, inhibition of adenosine triphosphate synthesis and increased generation of oxygen radicals. Therefore, an ideal silver-loaded material coating should completely inhibit microbial colonization, but allow for the normal adhesion and spreading of mammalian cells. For this purpose, it is necessary to have control over the concentration and release of the silver atoms from the coating.

In our earlier study (Bacakova *et al.,* 2008b), the composite Ag/hydrocarbon plasma polymer films were deposited on microscopic glass slides using an unbalanced planar magnetron with an Ag target (78 mm in diameter) operated in the dc mode in a working gas mixture of n-hexane and argon (pressure 2 Pa, deposition time 10 minutes, magnetron current 0.1 A). The concentration of silver was controlled by the ratio of n-hexane and argon in the working gas mixture. The concentration of silver in the films increased proportionally to the amount of Ar in the working gas mixture, ranging from 0 atomic % to 39 atomic % (i.e., 0, 3, 10, 30 and 39 atomic %), as estimated by RBS/ERDA.

On day 1 after seeding, the CPAE cells adhered to the films with 3 and 10 atomic % of Ag in similar numbers, and by similar cell spreading areas as on the control pure hydrocarbon plasma polymer films and glass slides. On day 3 after seeding, the cell numbers on pure hydrocarbon films, films with 3 atomic % of Ag and control glass coverslips reached similar values, only the cell number on films with 10 atomic % of Ag was significantly lower than on the pure hydrocarbon plasma polymer films. Nevertheless, on day 7 after seeding, the cells on pure hydrocarbon films, films with 10 atomic % of Ag and glass coverslips reached similar population densities, and on the films with 3 atomic % of Ag, this value was even significantly higher than on Ag-free films. The CPAE cells on films with 3 atomic % of Ag developed confluent layers of a cobblestone-like pattern, typical for mature endothelium, and contained well-apparent Weibel-Palade bodies with the von Willebrand factor, a marker of endothelial cell maturation. Moreover, immunofluorescence staining of the cells on films with 3 atomic % of Ag showed numerous and bright dot-like vinculin-containing focal adhesion plaques, which were even more apparent than on the control pure hydrocarbon plasma polymer films and glass (Fig. 1). Similar results were obtained in a rat mast cell line RBL-2H3 exposed to subtoxic concentrations of Ag^+ ions ranging from 10 to 100 μM, which induced degranulation and the release of histamine and leukotrienes via activation of focal adhesion kinase (Suzuki *et al.,* 2001). Adhesion of vascular endothelial cells was also enhanced on polystyrene implanted with Ag^- ions (Sato *et al.,* 1999). However, this effect seemed to be due to the degradation of the polymer by the ion bombardment followed by the polymer oxidation and the increase in its wettability, rather than due to a direct action of Ag^- ions entrapped in the polymer structure. Nevertheless, a moderate surface wettability of our surfaces with 3 atomic % of Ag (static water drop contact angle ~67°) could also

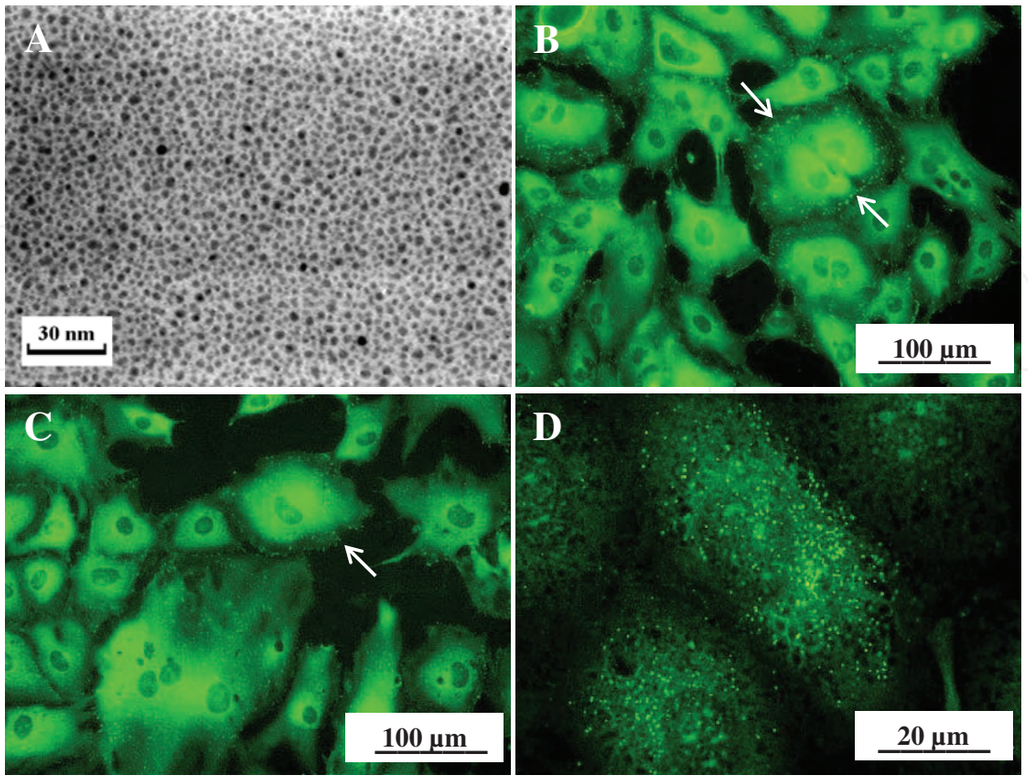

Fig. 1. Morphology of hydrocarbon plasma polymer composite films and their colonization with bovine pulmonary artery endothelial CPAE cells. A: Transmission electron micrograph of a film with 3 at.% of Ag. B, C: Immunofluorescence staining of vinculin, a protein of focal adhesion plaques (arrows), in CPAE cells on day 3 after seeding on films with 3 at.% of Ag (B) and 0 at.% of Ag (C). D: Immunofluorescence staining of von Willebrand factor, a marker of endothelial cell maturation in CPAE cells on day 3 after seeding on a film with 3 at.% of Ag. Olympus IX 51 microscope, DP 70 digital camera, obj. 20x and bar 100 µm (B, C), obj. 100x and bar 20 µm (D).

contribute to the good cell adhesion on these surfaces in our study (Bacakova *et al.*, 2008b). Another supportive factor was the nanoscale roughness of the Ag-containing surfaces. Transmission Electron Microscopy (TEM) revealed that Ag formed dark nanoclusters randomly dispersed in a lighter plasma polymer matrix (Fig. 1), and their diameter increased from 4 nm to 20 nm. However, at higher silver concentrations (30 and 39 atomic %), the supportive effects of the substrate nanostructure on its colonization with CPAE cells was disabled by the cytotoxicity of silver. On these films, the cells adhered at very low initial numbers, did not spread and usually died before day 7 of cultivation. As for the antibacterial effects of the silver-containing films, all these films, including those with the lowest Ag concentration (i.e., 3 atomic %), attenuated the growth of *E. coli.* The number of bacteria in wells (with glass coated with Ag-containing films) did not change significantly during 6 hours after inoculation, whereas the values on pure polystyrene dishes or on pure hydrocarbon polymer films increased by at least one order of magnitude after a 4-hour cultivation (Fig. 2). Similar results were obtained in a study by Vasilev *et al.*, (2010), performed on n-heptylamine plasma polymer (HApp) loaded with silver nanoparticles (at a concentration of 500 ng/cm^2) and coated with additional HApp films of various thicknesses, controlling the rate of release of silver atoms from the material. These films allowed for the

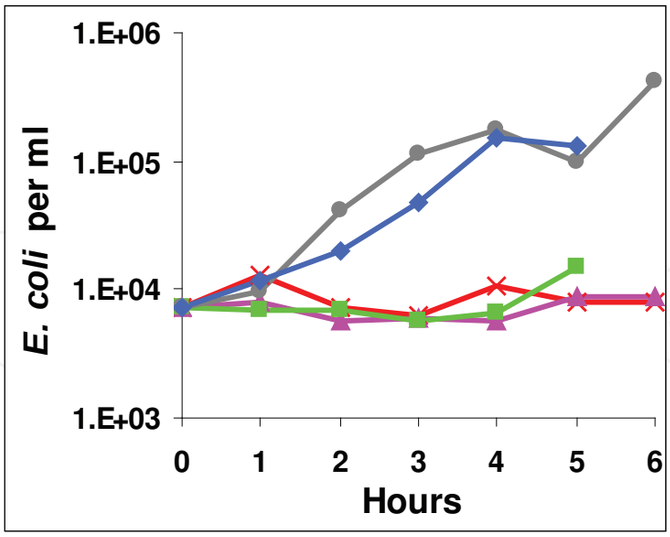

Fig. 2. Growth of *E. coli* on polystyrene dishes (blue), hydrocarbon plasma polymer films without Ag (gray), with 3 at.% Ag (green), with 30 at.% Ag (pink) or with 39 at.% Ag (red).

adhesion and growth of human SaOs-2 osteoblastic cells, while the colonization of the films with *Staphylococcus epidermidis* was markedly attenuated and even disabled.

However, it should be taken into account that for cultivation of mammalian cells, such as endothelial cells or osteoblasts, media supplemented with foetal bovine serum are used, while bacteria are usually incubated in a medium without serum. For example, in our study (Bacakova *et al.*, 2008b) an LB medium, containing bacto-tryptone (10 g/l), bacto-yeast extract (5g/l) and NaCl (10g/l) in H_2O was used. It has been reported that the serum supplement of the culture media has protective effects against the cytotoxic action of silver (Hidalgo *et al.*, 1998; Sun *et al.*, 2006). Thus, the promising results obtained in both studies by Bacakova *et al.* (2008b) and Vasilev *et al.* (2010) should be further investigated, particularly using the culture media of the same chemical composition for both mammalian and bacterial cells.

3. Amorphous carbon

Amorphous carbon, also referred to as diamond-like carbon (DLC; Tab. 1), possesses a number of favourable properties, such as high hardness, a low friction coefficient, chemical inertness and high corrosion resistance, which is due to its particular structure, i.e., cohabitation of the sp^2 and sp^3 phases (for a review, see Chai *et al.*, 2008). These properties make DLC, especially in the form of thin films, attractive for various biomedical applications, particularly for hard tissue surgery, such as orthopaedics and stomatology. For example, DLC has been deposited on the articular surfaces of artificial joint replacements (Santavirta 2003), dental prostheses or orthodontic archwires (Kobayashi *et al.*, 2007) in order to improve the resistance of these devices against wear, corrosion, debris formation and release of metallic ions, which can act as cytotoxic, immunogenic or even carcinogenic materials. In addition, due to their bioinertness, DLC films were also found to be suitable for cardiovascular applications, mainly as protective coatings of blood-contacting devices (intravascular stents, mechanical heart valves, pumps) in order to prevent hemocoagulation, thrombosis and inflammatory reaction on these surfaces (Monties *et al.*, 1994; Tran *et al.*, 1999; for a review, see Roy and Lee 2007).

However, DLC films can also act as bioactive substrates for the adhesion and subsequent growth of osteogenic cells, and thus they could be used as a protective coating for the bone-anchoring parts of joint prostheses, in which strong and quick integration with the surrounding bone tissue is required. In a study by Chai *et al.* (2008), DLC films were deposited on silicon substrates by Plasma-Enhanced Chemical Vapor Deposition (PECVD) using methane (CH_4) as a precursor gas. In order to improve their mechanical properties, some DLC films were deuterated, i.e., deposited using deuterated methane (CD_4) as a precursor gas. All surface treatments were performed under two different self-bias voltages (V_{sb}): -400 and -600V. DLC coatings prepared under the V_{sb} of -600V in pure methane ($600CH_4$) or in pure deuterated methane ($600CD_4$), significantly increased the proliferation rate of mouse osteogenic MC3T3-E1 cells compared to a pure Si substrate. Scanning Electron Microscopy (SEM) observations confirmed that the optimal cell adhesion behavior also occurred on the surface of the $600CH_4$ and $600CD_4$ groups of DLC, where the cells showed increased amounts of filopodia and microvilli, allowing a higher cell-environment exchange. Surprisingly, the mentioned DLC surfaces were relatively highly hydrophobic, having total surface energy and its polar component significantly lower than the values obtained on bare silicon substrates. It is generally accepted that the cell proliferation is optimal on moderately hydrophilic and polar surfaces, which enable adsorption of cell adhesion-mediating extracellular matrix molecules (such as vitronectin, fibronectin, collagen, laminin) in appropriate geometrical conformations, allowing accessibility of specific sites on these molecules to cell adhesion receptors (Chai *et al.,* 2008; Coelho *et al.,* 2010). In accordance with this proposition, the number and spreading of MG 63 cells was higher on micropatterned silicon substrates (grooves of 4, 8 and 10 μm in width) and coated with Ti, which were more hydrophilic and of a higher surface energy than the corresponding micropatterned substrates coated with DLC (Ismail *et al.,* 2007).

Also the addition of Ti into DLC films enhanced their attractiveness for cell colonization. In our earlier study (Bacakova *et al.,* 2001b), an amorphous carbon film enriched with Ti was used for coating carbon fiber-reinforced carbon composites (CFRC), i.e., a material which has been considered as promising for the construction of bone and dental implants. However, the surface roughness of CFRC is relatively high to enable optimal adhesion and growth of cells. As revealed by SEM, this was due to carbon fibers prominent over the carbon matrix. Another important problem is a tendency of CFRC to release particles, which is due to the relative brittle nature of the carbon matrix as well as carbon fibers. A possible solution of these problems may consist in covering the material surface with a mechanically resistant and highly biocompatible layer.

Therefore, CFRC were covered with a carbon-titanium layer, prepared by the PECVD method using unbalanced d.c. planar magnetron sputtering (2 x 4 kW, substrate temperature about 260°C) of a carbon poisoned titanium target in an acetylene-argon gas mixture at a total pressure of roughly 4×10^{-3} mbar. First, a metallic film (about 1 μm in thickness) was deposited by sputtering the metal target in pure argon and then C_2H_2 gas was added successively, giving a C:Ti film of at least 3.3 μm thickness. In this way, a layer consisting of a mixture of carbon and titanium atoms was created with an amorphous or very fine crystalline ("nanocrystalline") structure and with a gradually decreasing content of metal atoms from substrate to the surface. Clearly, the layer (and especially the layer surface) contains a large number of free bonds. These bonds cause strong adhesion of the layer to a substrate with a chemically very active surface.

The CFRC were then seeded with human osteoblast-like cells of the MG 63 line (passage 100) and vascular smooth muscle cells (i.e., another cell type present in the bone tissue), isolated

from the rat aorta (passage 9). On day 1 after seeding, both cell types adhered at higher numbers. From days 1 to 4 the cells exhibited shorter population doubling times. As a result, on day 4 after seeding, the cells attained higher population densities, volume and protein content. Since the surface roughness of CFRC was not significantly changed by the coating with the carbon-titanium layer, the beneficial effects of this coating on cell colonization could be explained by spontaneous oxidation of Ti and C in the cell culture system, including the formation of titanium oxides and oxygen-containing chemical functional groups. These features are known to enhance cell adhesion and growth (He *et al.,* 2008; Sawase *et al.,* 2008) and attract phosphate and calcium ions (Toworfe *et al.,* 2006; Rakngarm *et al.,* 2008), which facilitate bone tissue formation and bonding between the artificial implant and bone. Interestingly, the improvement of cell colonization by the C:Ti film was more pronounced in VSMC than in MG 63 cells, which was probably due to a different sensitivity of low-passaged cells and cell line to the physicochemical properties of the material surface. In addition, the release of carbon particles from the CFRC composites was significantly decreased (24 times) in the coated samples, and this effect was further enhanced by polishing the CFRC with colloidal SiO_2 (the particle release was decreased 42 times in polished + covered samples). Moreover, polishing the CFRC markedly improved the cell spreading on the material surface (Fig. 3). These results show that both polishing and carbon-titanium covering significantly improve the biocompatibility of CFRC composites *in vitro*, especially when these two modifications are combined (Bacakova *et al.,* 2001b).

Similar positive results were obtained in a study by Schroeder *et al.* (2000), where the hardness and inertness of a-C:H films were also combined with the biological acceptance of titanium. Different amounts of titanium of various concentrations, ranging from 7 to 24 atomic %, were incorporated into a-C:H films by a combined radio frequency (rf) and magnetron sputtering set-up. The X-ray Photoelectron Spectroscopy (XPS) of air-exposed a-C:H/Ti films revealed that the films were composed of TiO_2 and TiC embedded in and connected to an a-C:H matrix. Cell culture tests using primary bone marrow cells (BMC), derived from adult rat femora, revealed that the relative cell number, expressed as total DNA content per culture sample, was significantly increased on a-C:H with 10 and 13 atomic % of Ti compared with BMC cultures grown on glass. On all tested materials, i.e., a-C:H, a-C:H/Ti and control glass coverslips, BMC were able to differentiate to osteoblasts and osteoclasts, as revealed by measurements of the activity of alkaline phosphatase (ALP) and tartrate resistant acid phosphatase (TRAP), respectively. No significant differences in osteoblast differentiation on a-C:H, a-C:H/Ti and control glass coverslips were detected. However, the TRAP activity of osteoclast was lower on a-C:H with Ti than on the pure a-C:H. This decrease of osteoclast activity can be considered as a favourable result, i.e., an indicator for reduced inflammatory cell development (since osteoclast-like cells are derived from the monocyte family). Even in the form of particles added to BMC cultures, a-C:H and a-C:H/Ti did not significantly stimulate the osteoclast-related TRAP activity (Bruinink *et al.,* 2005). In addition, the Inductively Coupled Plasma Optical Emission Spectrometry (ICP-OES) measurements of culture media exposed to titanium containing a-C:H films showed that no titanium was dissolved from the films after one week under cell culture conditions (the detection limit for the ICP-OES method is 0.05 mg l^{-1}, i.e., 1.043 µmol l^{-1}; (Schroeder *et al.,* 2000). Thus, it can be concluded that a-C:H/Ti could be a valuable coating for bone implants by supporting bone cell proliferation, reducing osteoclast-like cell activation and bone resorption, and providing chemical stability to the implant surface.

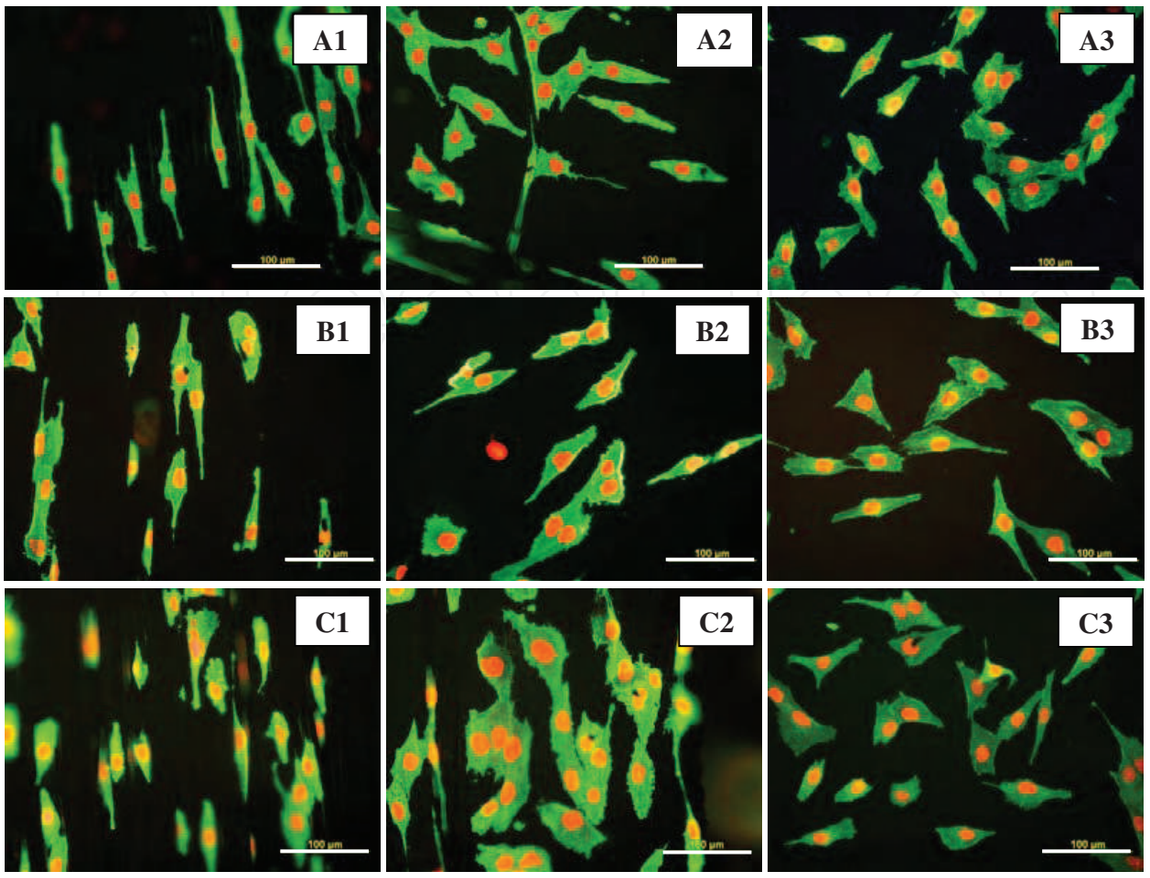

Fig. 3. Morphology of human osteoblast-like MG 63 cells on day 1 after seeding on control untreated CFRC composites (**A1**), CFRC composites ground by metallographic paper of 4000 grade (**A2**), CFRC composites ground with metallographic paper of 4000 grade, covered with pyrolytic graphite, ground by metallographic paper of 4000 grade and polished by diamond paste of 3/2 grade (**A3**). **B1, B2, B3** represent A1, A2, A3 covered with a-C:H, and **C1, C2, C3** are A1, A2, A3 covered with Ti-C:H layer. The cells were visualized by immunofluorescence staining of a cytoskeletal protein beta-actin, the nuclei were counterstained with propidium iodide. Olympus IX 51 microscope, obj. 20x, DP 70 digital camera, bar = 100 μm.

Also other C- and Ti-containing multicomponent coatings for load-bearing medical applications have been developed, such as the systems Ti-Ca-C-O-(N), Ti-Zr-C-O-(N), Ti-Si-Zr-O-(N) and Ti-Nb-C-(N). These films were deposited on various substrates, such as single crystal silicon (100), stainless steel, titanium alloy, glass coverslips and Teflon, by DC magnetron sputtering (atmosphere of Ar or mixture of Ar and N) from composite targets, which were manufactured by means of self-propagating high-temperature synthesis (Shtansky *et al.*, 2005). The films showed high hardness in the range of 30-37 GPa, significantly reduced Young's Modulus, low friction coefficient down to 0.1-0.2 and low wear rate in comparison with conventional magnetron-sputtered TiC and TiN films. The adhesion and proliferation of cultured cells (i.e., rat liver epithelial IAR-2 cells and Rat-1 embryonic fibroblasts), measured by cell numbers, were similar on all films and uncoated substrata. Only the cells cultivated on the Ti-Zr-C-O-(N) and Ti-Nb-C-(N) films disturbed

their actin cytoskeleton, which was manifested by the disappearance of circumferential actin bundles in IAR-2 cells and irregular short and thin actin bundles in the cytoplasma of Rat-1 fibroblasts. Nevertheless, the assessment of the population of cells covering the Teflon plates coated with the Ti-Ca-C-O-(N) and Ti-Zr-C-O-(N) films after 16 weeks of subcutaneous implantation into mice revealed a high biocompatibility level of tested films and the absence of inflammatory reactions (Shtansky *et al.*, 2005).

Other related materials promising for protective, tribological and load-bearing coatings of medical devices include nanostructured and nanocomposite binary (TiC-a:C), quaternary (Ti-B-C-N) and quinternary (Ti-Si-B-C-N) multicomponent films, prepared using unbalanced magnetron sputtering and closed field unbalanced magnetron sputtering from both elemental and composite targets (Lin *et al.*, 2009). Other nanocomposite films were based on nanocrystalline phases of metals and ceramics (Mo, Si, Al, Ti), embedded in an amorphous carbon matrix, and carbide-forming metal/carbon (Me/C) composite films (Me = Mo, W or Ti) deposited by a hybrid technique using Physical Vapor Deposition (PVD; magnetron sputtering) and PECVD, by the use of CH_4 gas (Teixeira *et al.*, 2009). Ti-TiC-TiC/DLC gradient films have been prepared by plasma immersion ion implantation and deposition (PIIID) combined with PECVD (Zheng *et al.*, 2008). All the mentioned films were usually characterized by excellent mechanical properties, particularly high hardness, low friction coefficient, high wear-resistance, improved adherence to the substrate and fracture toughness, corrosion resistance, and were constructed in order to overcome the limitations of pure DLC films.

4. Nanodiamond

From all nano-sized carbon allotropes, diamond (Tab. 1) can be considered as the most advantageous material for advanced biomedical and biosensoric applications, which is mainly due to the absence of its cytotoxicity, immunogenicity and other adverse reactions (Schrand *et al.*, 2007; Huang *et al.*, 2008; Grausova *et al.*, 2009a,b; Rezek *et al.*, 2009; for a review, see Bacakova *et al.*, 2008a). Other remarkable properties of nanodiamond, enabling its application in biotechnologies and medicine (particularly in hard tissue surgery), are high hardness, a low friction, and also high chemical, thermal and wear resistance. In our earlier studies and in studies by other authors, nanodiamond has proven itself as an excellent substrate for the adhesion, growth, metabolic activity and phenotypic maturation of several cell types *in vitro*, including osteogenic cells (Schrand *et al.*, 2007; Amaral *et al.*, 2008; Grausova 2008, 2009a,b; Kalbacova *et al.*, 2009). The beneficial effects of the nanodiamond layers on cell colonization lie in their nanoscale surface roughness (i.e., the size of irregularities less than 100 nm), which support the adsorption of cell-adhesion-mediating molecules in the appropriate geometrical conformation, enabling exposure of bioactive sites in these molecules (e.g., specific amino acid sequences such as RGD, KRSR etc.) to the cell adhesion receptors. In contrast, the adhesion of human osteoblasts was attenuated on microcrystalline diamond layers (Yang *et al.*, 2009).

The nanodiamond layers also acted as suitable platforms for the adhesion of mammalian neurons, neurite outgrowth and the formation of excitable neuronal networks *in vitro*, which have great potential for chronic medical implants (Thalhammer *et al.*, 2010). In studies *in vivo*, diamond layers, deposited on Ti6Al4V probes and implanted into a rabbit femur, showed very high bonding strength to the metal base as well as to the surrounding bone tissue, and prevented material corrosion (Rupprecht *et al.*, 2002). Nanocrystalline and

multilayer diamond thin films were also used for coating the heads and cups of an artificial temporomanibular joint made of Ti6Al4V alloy (Papo *et al.,* 2004). Another advantageous property of diamond and/or nanodiamond is its ability to bind various biological molecules, which can be utilized for sensing, detecting, separating and purifying these molecules (Bondar *et al.,* 2004; Kong *et al.,* 2005; Rezek *et al.,* 2007).

Nanocrystalline diamond (NCD) films used in our earlier studies also proved to be an impermeable coating preventing adverse effects of the underlying substrate on cell colonization. For deposition of NCD films (Kromka *et al.,* 2008), we used (100) oriented silicon substrates. Uncoated substrates acted cytotoxically on human osteoblast-like MG 63 cells and bovine pulmonary artery endothelial CPAE cells. On day 1 after seeding, both cell types adhered to silicon substrates in significantly lower numbers than on NCD films, control polystyrene dishes and microscopic glass coverslips. On day 5 after seeding, no MG 63 cells and few CPAE cells were detected on these substrates, while the cells on NCD films grew to similar cell population densities as on the reference polystyrene dishes and glass (Grausova *et al.,* 2008).

An interesting issue is doping of NCD films with boron. This doping renders the NCD films electroconductive (Gajewski *et al.,* 2009). Boron-doped NCD films have been applied in electronics and sensorics, e.g., for the construction of sensors for DNA hybridization (Nebel *et al.,* 2007), bacteria (Majid *et al.,* 2008) or glucose (Zhao *et al.,* 2009). However, little is known about the influence of boron-doped NCD films on the adhesion, growth, differentiation and function of osteogenic cells, and thus on their potential use as a substrate for bone tissue regeneration.

In our earlier studies, the nanocrystalline diamond films (NCD) were deposited on glass (Kopecek *et al.,* 2008) or silicon substrates (Kromka *et al.,* 2010) by a microwave plasma-enhanced CVD process. Boron doping was achieved by adding trimethylboron (TMB) to the gas mixture, and the B:C ratio varied from 100 to 6700 ppm. The study by Kromka *et al.* (2010) revealed that the increase in the number of human osteoblast-like MG 63 cells in 7-day-old cultures was most apparent on NCD doped with 133 and 1000 ppm of B than on films with 6700 ppm of B. At the same time, the cells on NCD with 6700 ppm of B developed large and numerous focal adhesion plaques containing talin (Fig. 4), and contained the highest concentration of focal adhesion protein vinculin. Both features are indicators of firm cell-substrate adhesion, which was probably enabled by the flattest appearance of the nanodiamond crystals on films doped with 6700 ppm of B. It has been reported that cell proliferation activity is the highest at intermediate cell-substrate adhesion strength (for a review, see Bacakova *et al.,* 2004; Bacakova and Svorcik 2008). If this strength is relatively high, the cells slow down their proliferation activity and enter the differentiation program. In accordance with this, the cells on NCD films doped with 6700 ppm of B contained one of the highest concentrations of osteocalcin (i.e., a calcium-binding non-collagenous ECM protein and an important marker of osteogenic cell differentiation), which was significantly higher than the value on non-doped NCD and on the control polystyrene cell culture dishes. Similar results were also obtained in the study by Kopecek *et al.* (2008) performed on NCD films doped with 3000 ppm of B, where MG 63 cells were less numerous on boron-doped NCD films than on non-doped NCD films, but they were more intensely immunofluorescently stained against osteocalcin.

The beneficial effects of boron-doping on cell colonization of NCD films can be attributed to the electroactivity of these films. The electrical resistivity of the films decreased from >100 MΩ (non-doped films) to 100, 2, and 0.4 kΩ in films doped with 133, 1000 and 6700 ppm of

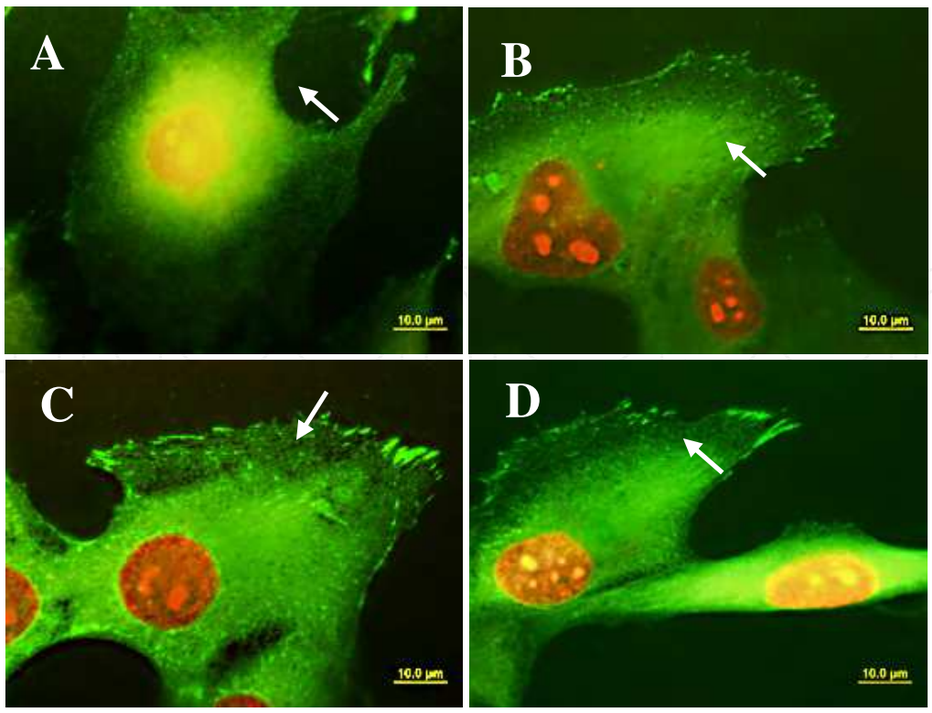

Fig. 4. Immunofluorescence staining of talin in MG 63 cells on day 3 after seeding on non-doped NCD (**A**), NCD films doped with boron in concentrations of 133 ppm (**B**), 1000 ppm (**C**) and 6700 ppm (**D**). The cell nuclei were counterstained with propidium iodide. Olympus IX 51 epifluorescence microscope, DP 70 digital camera, obj. 100x, bar = 10 µm.

B. In addition, Kelvin Force Microscopy revealed that the surface potential of NCD films increased proportionally to the boron concentration, i.e., from +19 ± 10 mV in non-doped films to +27 ± 26 mV, +112 ± 19 mV and +97 ± 34 mV in films with 133, 1000 and 6700 ppm of B, respectively (Kromka *et al.,* 2010). It is known that electroactive surfaces stimulate the adhesion, growth and specific functions of cells even without their active stimulation with electrical current. For example, Schwann cells cultured on electrically conductive melanin films accelerated their proliferation, and rat pheochromocytoma PC12 cells enhanced extension of their neurites (Bettinger *et al.,* 2009). Similarly, composite nanofibers made of electrically conductive polyaniline blended with poly(L-lactide-co-epsilon-caprolactone) enhanced the adhesion and proliferation of C2C12 murine skeletal muscle myoblasts, as well as their differentiation towards myotubes (Jeong *et al.,* 2008; Jun *et al.,* 2009).
The mechanisms of the positive effects of electroactive materials on cell colonization and function (which can be further enhanced by additional electrical stimulation of cells through the materials) have not yet been fully elucidated and systemized. These mechanisms probably include enhanced adsorption of cell adhesion-mediating ECM proteins from biological environments, a more advantageous geometrical conformation of these proteins for their accessibility by cell adhesion receptors, redistribution of cell membrane growth factors and adhesion receptors or cytoskeletal proteins such as actin, activation of ion channels in the cell membrane, followed by cell depolarization, hyperpolarization or generation of action potential, movement of charged molecules inside and outside the cell, upregulated mitochondrial activity and enhanced protein synthesis (for a review, see (Schmidt *et al.,* 1997; Gomez *et al.,* 2007; Khang *et al.,* 2008; Shi *et al.,* 2008).

Another factor contributing to better performance of MG 63 cells on B-doped films could be the slightly increased RMS surface roughness of these films (RMS from 25 to 30 nm versus 19 nm on non-doped films; Kromka *et al.,* 2010). Similarly, in a study by Kalbacova *et al.* (2007), the metabolic activity of SaOs-2 osteoblasts, measured by the activity of dehydrogenases in these cells, increased with increasing surface roughness of O-terminated NCD films (RMS from 11 to 39 nm). Direct action of boron on the cell metabolism is less probable, because boron atoms are strongly bound in the NCD lattice or around the grain boundaries, and their release is very limited, even at very high temperatures combined with a vacuum and a strong electrical field, i.e., conditions not occurring in biological environments (for a review, see Kopecek *et al.,* 2008).

All these results indicate that the NCD films provided very good supports for colonization with osteogenic cells. The potential of these films for bone tissue regeneration can be further enhanced by boron-doping, which can be explained by the electroactivity (i.e., electrical conductivity and changes of surface electrical potential) of boron-doped NCD films.

Boron-doped diamond films have also been used for the construction of patterned surfaces for regionally-selective adhesion and guided growth of cells. In a recent study by Marcon *et al.* (2010), the boron-doped polycrystalline diamond was prepared from a $B_2H_6/CH_4/H_2$ source gas mixture by Hot Filament-Assisted Chemical Vapour Deposition (HFCVD). These substrates were then patterned with stripe-like hydrophilic microdomains with oxygen containing chemical functional groups or amine groups (water drop contact angle of 4° and 53°, respectively) and hydrophobic microdomains terminated with hydrogen or methyl-, trifluoromethyl- and vinyl- groups (contact angle from 92° to 114°). Human osteosarcoma U2OS and mouse fibroblast L929 cells preferentially colonized the hydrophilic domains, forming confluent arrays with distinguishable edges separating the hydrophobic alkyl regions. Similar results were obtained with human osteosarcoma SaOs-2 cells in cultures on NCD films patterned with hydrophilic O-terminated and hydrophobic H-terminated domains (Kalbacova *et al.,* 2008). The micropatterned diamond-based surfaces have a great potential for the development of biosensors, biostimulators, construction of cell microarrays for advanced genomics and proteomics and also for tissue engineering. In addition, the size and shape of the adhesive domains can be utilized for regulation of the cell spreading, which has a strong influence on further cell behaviour, e.g., switching between apoptosis and proliferation or proliferation and differentiation programs (for a review, see Bacakova *et al.,* 2004; Bacakova and Svorcik 2008).

5. Graphite

Graphite is one of the most common allotropes of carbon (named by Abraham Gottlob Werner in 1789 after the Greek word graphein, i.e., "to draw/write", for its use in pencils). Graphite is the most stable form of carbon under standard conditions; it is an electrical conductor, and can be used, for instance, as the material in the electrodes of an electrical discharge. However, despite its electrical conductivity, which is usually associated with the stimulatory effects on cell colonization and functioning, unmodified graphite is rather bioinert, i.e., less adhesive for cells (Watari *et al.,* 2009). It is due to a relatively low ability of graphite to adsorb cell adhesion-mediating proteins from the serum supplement of the culture medium (Aoki *et al.,* 2007; Li *et al.,* 2009a) and also bone morphogenetic proteins (BMP), such as BMP-2, a factor promoting the osteogenic cell differentiation (Li *et al.,* 2009b). As a result, graphite compacts allowed the attachment of mouse myoblastic C2C12 cells in significantly lower numbers compared to

carbon nanotube compacts, which showed a significantly high capability to adsorb proteins. The C2C12 cells then proliferated more slowly, and contained a lower amount of alkaline phosphatase and total protein (Li *et al.,* 2009a). A similar response was found in human osteosarcoma SaOs-2 cells, which attached and proliferated much worse on graphite than on single- and multi-walled carbon nanotube films (Aoki *et al.,* 2007). In addition, SaOs-2 cells cultured on graphite showed a lower expression of osteonectin, osteopontin and osteocalcin, i.e., markers of osteogenic cell differentiation, and a lower content of alkaline phosphatase and total protein after pre-soaking both graphite and nanotube compacts in the culture medium with BMP-2 (Li *et al.,* 2009b).

In our earlier studies, graphite was prepared by pyrolysis, i.e., by a process defined as thermochemical decomposition of organic material at elevated temperatures (above 430 °C) in the absence of oxygen. However, in practice it is not possible to achieve a completely oxygen-free atmosphere. Because some oxygen is present in any pyrolysis system, a small amount of oxidation occurs. In our experiments, carbon fiber-reinforced carbon composites (CFRC) were coated with pyrolytic graphite by decomposition of butane in a mixture with N_2 at a pressure of 4 Pa, a temperature of 1900 °C and for 300–400 minutes. This coating increased the number of human osteoblast-like MG 63 cells on days 1 and 3 after seeding, and shortened the cell population doubling time compared to uncoated composites (Stary *et al.,* 2002). These results could be attributed to the presence of oxygen-containing chemical functional groups (e.g., hydroxyl, carbonyl, carboxyl) on the pyrolytic graphite films (Stary *et al.,* 2003). It is known that these groups promote cell adhesion and growth by increasing the polarity, and wettability of the material and thus its attractiveness for adsorption of cell-adhesion mediating molecules (Bacakova *et al.,* 2001a). At the same time, the surface roughness and topography, measured by the parameters R_a (departures of the roughness profile from the mean line), R_q (root mean square deviation of the assessed profile) and S (the mean spacing of the adjacent local peaks), was not significantly changed by coating CFRC by pyrolytic graphite (Stary *et al.,* 2002, 2003).

Graphite has also been used in three-dimensional systems as a component of various composite materials used for construction of bone implants. For example, carbon/graphite fibers were used for reinforcing poly(methylacrylate) implants designed for reconstruction of the maxilla damaged by malignant tumors (Ekstrand and Hirsch 2008). Graphite fibers were also applied for reinforcing of polyetheretherketone (PEEK) for construction of composite hip joint prostheses (Yildiz *et al.,* 1998a,b).

Unlike some other carbon allotropes, namely fullerenes and nanotubes, graphite is not cytotoxic. The cell viability tests, performed on human epithelial L132 cells (colony-forming method) and mouse osteoblast-like MC3T3-E1 cells (staining with Blue Alamar dye) showed excellent cytocompatibility of graphite powder (Hornez *et al.,* 2007). Only pyrolytic carbon (i.e., carbon more or less similar to graphite prepared by pyrolysis, which has lost its lubrication properties due to a large number of crystallographic defects), showed some tendency to induce inflammatory or hyperplastic reactions. Coating polyethylene terephthalate (PET) with pyrolytic carbon induced expression of mRNAs specific for platelet-derived growth factors (PDGF-A, PDGF-B) and transforming growth factors (TGF-β1 and TGF-β2) in human umbilical vein endothelial cells (HUVEC) cultured on this substrate, but did not change expression of mRNA for interleukin-6 (Cenni *et al.,* 2000). As determined by flow cytometry, pyrolytic carbon coating on PET did not increase the percentage of cells positive for platelet endothelial cell adhesion molecule-1 (PECAM-1), endothelial leukocyte adhesion molecule-1 (ELAM-1), intercellular adhesion molecule-1

(ICAM-1) and vascular cell adhesion molecule-1 (VCAM-1), nor the intensity of fluorescence of these molecules (Cenni *et al.,* 1995). However, in experiments *in vivo*, pyrolytic carbon and pyrolytic graphite/silicon-carbide, implanted into rabbit mandibles, induced fibrous capsule formation and infiltration with multinucleated phagocytic cells (Maropis *et al.,* 1977). On the other hand, similarly as the amorphous hydrogenated carbon, pyrolytic carbon (particularly in the form of so-called Low Temperature Isotropic pyrolytic carbon, LTI) has been used as a coating for commercially available blood contacting devices, such as artificial heart valves (Kwok *et al.,* 2004; Jackson *et al.,* 2006), in order to prevent hemocoagulation and thrombus formation on these devices, although its hemocompatibility was not ideal. LTI has been also used in orthopedic applications, namely for construction of joint replacements, because it has been reported to reduce the cartilage wear (Bernasek *et al.,* 2009). In addition, when deposited on CFRC composites, pyrolytic carbon supported proliferation of embryonal human lung fibroblasts of the line LEP, particularly if the composites were polished after coating (Pesakova *et al.,* 2000). Also in our studies performed on CFRC, coating with pyrolytic graphite combined with polishing the material surface increased spreading and subsequent growth of human osteoblast-like MG 63 cells (Stary *et al.,* 2002, 2003; Figs. 3, 5)

6. Fullerenes

Fullerenes were discovered, prepared and systemized by Kroto *et al.* (1985). These spheroidal molecules are made exclusively of carbon atoms (e.g., C_{60}, C_{70}) and display a diverse range of biological activity. Their unique hollow cage-like shape and structural analogy with clathrin-coated vesicles in cells support the idea of the potential use of fullerenes as drug or gene delivery agents. For example, a fullerene derivative, namely bisphosphonate fullerene $C_{60}(OH)_{16}$AMBP, i.e., (4,4-bisphosphono-2-(polyhydroxyl-1,2-dihydro-1,2-methanfullerene$_{60}$-61-carboxamido) butyric acid) has been shown to have a strong affinity for the bone tissue, which is due to binding sites of this compound for hydroxyapatite. Thus, this bone-vectored fullerene derivative could be used as a carrier for radionuclides or other drugs for selective therapy of bone tumors (Gonzales *et al.,* 2002).
Other biological activities of fullerenes arise from their reactivity, due to the presence of double bonds and bending of sp^2-hybridized carbon atoms, which produces angle strain. Fullerenes can act either as acceptors or donors of electrons. When irradiated with ultraviolet or visible light, fullerenes can convert molecular oxygen into highly reactive singlet oxygen. Thus, they have the potential to inflict photodynamic damage on biological systems, including damage to cellular membranes, inhibition of various enzymes or DNA cleavage. This harmful effect can be exploited for photodynamic therapy against tumors (Liu and Tabata 2010), viruses including HIV-1 (Marchesan *et al.,* 2005) and broad spectrum of bacteria and fungi (Huang *et al.,* 2010). On the other hand, C_{60} is considered to be the world's most efficient radical scavenger. This is due to the relatively large number of conjugated double bonds in the fullerene molecule, which can be attacked by radical species. Thus, fullerenes would be suitable for applications in quenching oxygen radicals, and thus preventing inflammatory and allergic reactions (Dellinger *et al.,* 2009) and damage of various tissues and organs, including the lung (Chen *et al.,* 2004), blood vessels (Maeda *et al.,* 2008) and brain (Tykhomyrov *et al.,* 2008; Lao *et al.,* 2009). Fullerenes also protected epithelial cells *in vitro* from anoikis, i.e., apoptosis due to adhesion deprivation, by a mechanism supporting the formation of focal adhesion plaques, assembly of the actin cytoskeleton and cell spreading, which was also attributed to the antioxidative action of fullerenes (Straface *et al.,* 1999).

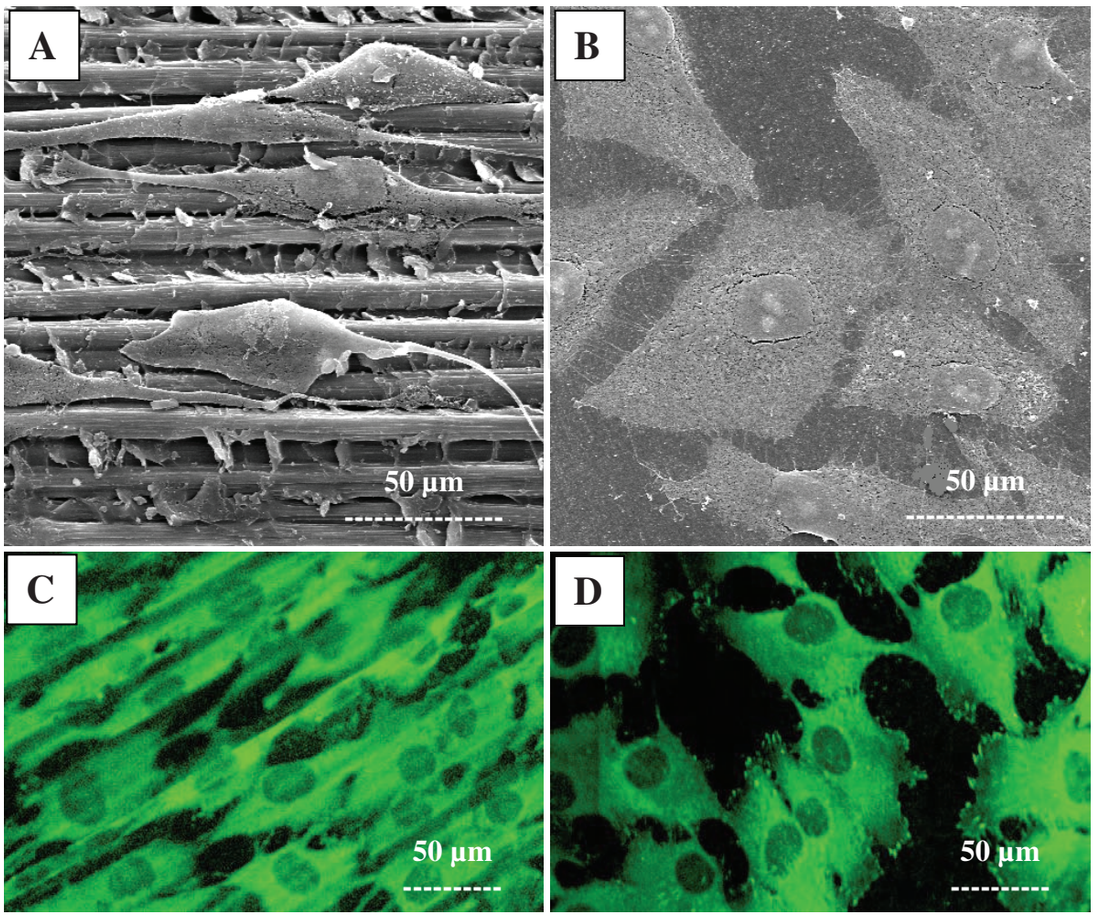

Fig. 5. Morphology of human osteoblast-like MG 63 cells on pristine CFRC composites (**A, C**) and composites ground with metallographic paper, coated with pyrolytic graphite, again ground with metallographic paper and polished with diamond paste 3/2 (**B, D**). Note that on pristine unmodified composites, the cells are spindle-shaped, arranged in parallel to carbon fibers prominent on the surface (**A**), and do not contain distinguishable vinculin-containing focal adhesion plaques (**C**), while on modified composites, the cells are well-spread, polygonal (**B**) and with clearly developed vinculin-containing focal adhesion plaques (**D**). **A, B**: scanning electron microscope JSM5410, JEOL, Japan, day 1 after seeding; **C, D**: Immunofluorescence of vinculin, an integrin-associated focal adhesion protein, in cells on day 4 after seeding, Bio-Rad MRC600 confocal laser scanning microscope, oil immersion 60× objective, (numerical aperture = 1.4), excitation wavelength 488 nm.

Recently, several derivatives of fullerenes C_{60} were synthesized, e.g., glutathione C_{60}, beta-alanine C_{60}, cystine C_{60} or folacin C_{60} (Hu *et al.*, 2007a,b,c; 2010), and were proven to have a protective activity against oxidative stress in rat pheochromocytoma PC12 cells, induced by treatment of these cells with hydrogen peroxide and leading to apoptotic death of unprotected cells.

In addition, fullerenes emit photoluminescence which could be utilized in advanced imaging technologies for diagnostics of various diseases, e.g., cancer (Levi *et al.*, 2006). For a more detailed review of biological effect of fullerenes and their derivatives, see our earlier studies (Bacakova *et al.*, 2008a, Grausova *et al.*, 2009c).

Our earlier studies were focused on fullerenes deposited in the form of thin films for cell cultivation, because relatively little is still known about the behaviour of cells when fullerenes act as their growth supports. For this purpose, fullerenes C_{60} (purity 99.5 %, SES Research, USA) were deposited onto microscopic glass coverslips by evaporation of C_{60} in the Univex-300 vacuum system (Leybold, Germany) in the following conditions: room temperature of the substrates, C_{60} deposition rate ≼1 Å/s, temperature of C_{60} evaporation in the Knudsen cells about 450° C. The thickness of the layers increased proportionally to the temperature in the Knudsen cell and the time of deposition. As revealed by AFM, the layer thickness was 505 ± 43 nm and 1090 ± 8 nm. The Raman spectroscopy showed that the fullerene films were prepared with high quality, i.e., without fragmentation and graphitization. After sterilization of the fullerene films with ethanol, which was necessary for cell cultivation, some of the C_{60} molecules reacted with oxygen or polymerized (Grausova *et al.,* 2009c,d).

The fullerene-coated glass coverslips were then inserted into 24-well polystyrene multidishes (TPP, Switzerland), seeded with human osteoblast-like MG 63 cells and incubated in Dulbecco's modified Eagle's Minimum Essential Medium supplemented with 10% fetal bovine serum. On day 1 after seeding, the cells on both thin and thick fullerene layers adhered at similar numbers, comparable to the values found on standard cell culture substrates, represented by the tissue culture polystyrene dishes and microscopic glass coverslips. However, the cell spreading area (i.e., the cell area projected on the material) was significantly smaller on both thin and thick fullerene films, which could be attributed to a relatively high hydrophobicity of these films (sessile water drop contact angle from 97 ± 2° to 101 ± 7°). Nevertheless, between days 1 to 5 after seeding, the cells on both thin and thick C_{60} films proliferated with similar and relatively short cell population doubling times (about 19 hours) as the cells on polystyrene and glass, and on day 5, the cells on all tested substrates reached similar cell population densities. The cells on the fullerene layers were of normal polygonal or spindle-like shape, they were homogeneously distributed on the material surface and on day 7 after seeding, they practically reached confluence (Grausova *et al.,* 2009c; Fig. 6).

Thus, the fullerene C_{60} layers in our study were colonized with human osteoblast-like MG 63 cells to a similar extent as standard cell culture polystyrene dishes. We considered this result rather surprising, because many studies have reported cytotoxic and even genotoxic effects of fullerenes (Xu *et al.,* 2009; Johnson-Lyles *et al.,* 2010; for a review, see Bacakova *et al.,* 2008a). However, the cytotoxic action of fullerenes was usually associated with suspending fullerenes in the cell culture medium (Yamawaki *et al.,* 2006; Gelderman *et al.,* 2008) or UV-light irradiation (Prylutska *et al.,* 2010), while our fullerene layers were resistant to be dissolved in a water environment, and the cells were cultured in the dark. In addition, the cytotoxic effects of fullerenes are based mainly on the reactivity of fullerenes, which may weaken with time due to the oxidation and polymerization of fullerenes in an air atmosphere, ethanol or cell culture medium, as revealed by Raman spectroscopy.

Similarly as in other carbon-based thin films described in this review, the supportive effect of fullerene layers on cell colonization could also be explained by their surface nanostructure, mimicking the nanoarchitecture of the natural ECM, i.e., a physiological substrate for cell adhesion. In addition, the cell colonization could be supported by the presence of oxygen, revealed by Raman spectroscopy. Both the nanostructure and the oxygen content in our C_{60} layers may act synergetically by improving the adsorption of cell

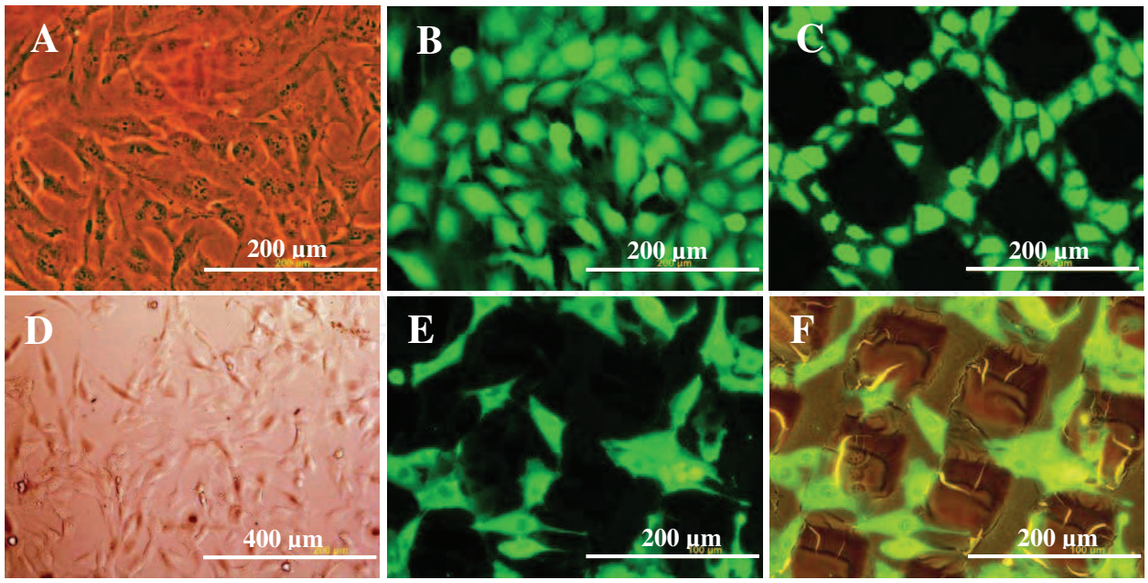

Fig. 6. Human osteoblast-like MG 63 cells in cultures on continuous and micropatterned C_{60} and C_{60}/Ti films. **A-C**: Cells on day 7 after seeding on a continuous fullerene C_{60} layer (505 ± 43 nm in thickness, **A**), and micropatterned C_{60} layers with prominences 128 ± 8 nm in height (**B**) or 1043 ± 57 nm in height (**C**). **D-F**: Cells on day 3 after seeding on a continuous C_{60}/Ti film (274 ± 11 nm in thickness, **D**) and micropatterned C_{60}/Ti layer with prominences 351 ± 18 nm in height (**E, F**). **A, D**: Native cells without staining; **B, C**: Cells stained with LIVE/DEAD viability/cytotoxicity kit; **E, F**: Cells visualized by immunofluorescence of β-actin. **E**: Fluorescence only, **F**: Combination of fluorescence and conventional light in order to visualize the grooves among the prominences. Olympus IX 51 microscope, DP 70 digital camera, obj. 20x and bar = 200 µm (except **D** where obj. is 10x and bar = 400 µm).

adhesion-mediating ECM molecules, such as vitronectin, fibronectin and collagen, provided by the serum of the culture medium or synthesized by the cells. The spatial conformation of these molecules on our films may also be more appropriate for the accessibility of specific sites on these molecules by cell adhesion receptors.

In our studies, fullerenes C_{60} were also deposited on microscopic glass coverslips in the form of micropatterned layers, i.e., through a metallic mask with rectangular holes (Grausova *et al.*, 2009c,d). Proportionally to the increasing temperature and the time of deposition, the thickness of the layers on sites underlying the openings of the grid was 128 ± 8 nm, 238 ± 3 nm, 326 ± 5 nm and 1043 ± 57 nm (data presented as mean ± standard deviation). Fullerene layers were also formed below the metallic part of the grid, where their thickness was usually within the size of the standard deviation. Thus, the fullerene layers contained bulge-like prominences separated by grooves.

From day 1 to 7 after seeding, the cells on the layers with the fullerene prominences of 128 ± 8 nm, 238 ± 3 nm and 326 ± 5 nm were distributed almost homogeneously over the entire material surface. Thus, the cell population densities on the prominences and in the grooves, and also the total cell population densities on all three surfaces, were similar. However, the cells on the layers with prominences of 1043 ± 57 nm were found preferentially in the grooves (Fig. 6). These grooves contained from 75.0 ± 13.4 % to 99.6 ± 0.3 % of cells, although they occupied only 44 ± 3 % of the material surface. The cell population density in the grooves was about 5 to 192 times higher than on the bulges, and these differences increased with time of cultivation.

On various polymeric, metallic or carbon-based materials, the cells were usually able to colonize the prominences on these surfaces, although these prominences amounted to several micrometers or even tens of μm (for a review, see Bacakova *et al.,* 2008a; Grausova *et al.,* 2009c,d). Surprisingly, on our fullerene C_{60} layers, the MG 63 cells were not able to "climb up" relatively low prominences (i.e., only about 1 μm in height), even at a relatively late culture interval of 7 days after seeding. This may be due to a synergistic action of certain physical and chemical properties of the fullerene bulges less appropriate for cell adhesion, such as their hydrophobicity, a steep rise as well as the tendency of spherical ball-like fullerene C_{60} molecules to diffuse out of the prominences (Guo *et al.,* 2007).

In our studies, hybrid C_{60}/Ti layers were also formed by co-deposition of C_{60} molecules and Ti atoms in an ultra-high vacuum (UHV) chamber (background pressure of ~10^{-7} Torr) using the Knudsen cell and electron gun for vaporization of C_{60} and Ti, respectively. Ti was chosen as a highly biocompatible metal often used for the construction of bone implants. Its concentration in the layers varied from about 25% to 75%, i.e., from 25 to 75 Ti atoms per 75 to 25 C_{60} molecules. Similarly to pure C_{60} films, hybrid C_{60}/Ti layers also promoted the adhesion and growth of MG 63 cells in a similar or even higher extent compared to standard polystyrene culture dishes and microscopic glass coverslips, and when deposited in micropatterned form, they induced regionally-selective cell adhesion and growth of these cells in grooves among the prominences (Vandrovcova *et al.,* 2008; Vacik *et al.,* 2010; Fig. 6).

At the same time, potential DNA damage by the hybrid C_{60}/Ti films was analyzed by immunofluorescence staining of markers of DNA damage response, such as phosphorylation of histone H2AX (Bekker-Jensen *et al.,* 2006) and focal recruitment of p53-binding protein (Schultz *et al.,* 2000). H2AX is a member of the histone H2A family. The formation of nuclear double-strand breaks (DSBs) triggers phosphorylation of H2AX at Ser139, referred as gamma-H2AX. Phosphorylation of H2AX is the first step in recruiting and localizing DNA repair proteins. The combination of phosphospecific antibodies, which recognize the phosphorylated Ser139 residue of gamma-H2AX, with immunofluorescence microscopy document the local phosphorylation through the formation of distinct foci in the vicinity of DSBs and allow for monitoring of their induction and repair. Another important protein involved in DNA repair is the p53 binding protein 1 (53BP1). Efficient 53BP1 focal recruitment depends on a number of upstream factors, including phosphorylation of H2AX at Ser139, recruitment of other mediator proteins (such as MDC1 and the E3 ubiquitin ligase RNF8), methylation of histones H3 and H4 and Tip60 HAT (histone acetyltransferase) activity, which can acetylate histone residues and therefore may facilitate 53BP1 recruitment through the formation of a more open chromatin structure. However, it is important to note that gamma-H2AX is not required for the initial recruitment of 53BP1 immediately following DNA damage.

As a positive control to the markers of DNA damage response, a 7-day-long treatment with 2.5 mM thymidine was used. The proliferation activity and morphological changes of the cells were also monitored. After 7 days of cultivation, we observed no cytotoxic morphological changes, such as enlarged cells or cytosolic vacuole formation, which are signs of cell senescence, and no increased induction of cell death. In addition, there was no increased level of DNA damage response on the C_{60}/Ti composites. We also found no significant differences in cell population densities and no increased level of DNA damage among various Ti concentrations (Kopova *et al.,* 2010). These results suggest that fullerenes, in combination with Ti, do not cause cytotoxic injury, and thus this material could be used for coating bone implants. However, Raman spectroscopy revealed that most fullerene

molecules were disintegrated by their co-deposition with Ti, and converted to amorphous carbon (a-C). In addition, the hybrid C_{60}/Ti films also contained polymerized and oxidized structures (Vandrovcová *et al.,* 2008; Vacík *et al.,* 2010).

7. Carbon nanotubes

Carbon nanotubes are, in comparison with other carbon allotropes, relatively newly discovered carbon nanoparticles, which were first described, synthesized and systemized by Iijima (Iijima and Ichihashi 1993; Iijima 2002). These tubular structures are formed by a single cylindrically-shaped graphene sheet (single-wall carbon nanotubes, usually referred to as SWNT or SWCNT) or several graphene sheets arranged concentrically (multi-wall carbon nanotubes, referred to as MWNT or MWCNT). Carbon nanotubes have excellent mechanical properties, mainly due to sp^2 bonds. The tensile strength of single-walled nanotubes is about one hundred times higher than that of the steel, while their specific weight is about six times lower (Iijima and Ichihashi 1993; Yakobson *et al.,* 1997; Iijima 2002). Thus, carbon nanotubes could be utilized in hard tissue surgery, e.g., to reinforce artificial bone implants, particularly scaffolds for bone tissue engineering made of relatively soft synthetic or natural polymers. Carbon nanotubes have been used in combination with poly(carbonate) urethane (Khang *et al.,* 2007, 2008), biodegradable polymers such as polylactic acid (Supronowicz *et al.,* 2002), propylene fumarate (Shi *et al.,* 2006), poly(3-hydroxybutyrate) (Misra *et al.,* 2010), a copolymer of polylactide-caprolactone (Lahiri *et al.,* 2009) or a copolymer of polypyrrole-hyaluronic acid (Pelto *et al.,* 2010). Also hydroxyapatite (HAp), i.e., a ceramic material widely used in bone tissue engineering, but known for its high brittleness, has been reinforced with carbon nanotubes (Balani *et al.,* 2007; Hahn *et al.,* 2009). Carbon nanotubes not only improved the mechanical properties of the mentioned materials, such as tensile (Young's) modulus, compressive and flexural moduli and compressive, flexural and tensile strength in the polymeric materials (Shi *et al.,* 2006; Lahiri *et al.,* 2009; Misra *et al.,* 2010), and fracture toughness, hardness, elastic modulus and adhesion to the underlying substrate in HAp coatings (Balani *et al.,* 2007; Hahn *et al.,* 2009), but also increased the attractiveness of these materials for the adhesion, growth, differentiation and phenotypic maturation of cells, such as osteoblasts, chondrocytes and stem cells. One of the mechanisms of the improved cell colonization was an increased adsorption of fibronectin, i.e., an important cell-adhesion mediating ECM protein, to these composites, which has been explained by creating a nanoscale surface roughness of the material by the addition of nanotubes, and also by an increased material surface hydrophilia due to the presence of the polymeric component (pure carbon nanotube surfaces were highly hydrophobic, Khang *et al.,* 2007, 2008). Another important mechanism is the electroactivity of carbon nanotubes, i.e., their electrochemical activity, electrical charge and conductivity, which enable electrical stimulation of cells (Supronowicz *et al.,* 2002; Zanello *et al.,* 2006; Khang *et al.,* 2008; Pelto *et al.,* 2010). For example, osteoblasts cultured on nanocomposites consisting of polylactic acid and carbon nanotubes and exposed to electrical stimulation (current 10 μA, frequency 10 Hz), increased their proliferation activity, concentration of extracellular calcium and mRNA expression for collagen type I (Supronowicz *et al.,* 2002). Similarly, human chondrocytes cultured on MWCNT/poly(carbonate) urethane composites (weight ratio 1:2) and subjected to electrical stimulation (current 10 μA, frequency 10 Hz) adhered to these substrates in higher numbers and reached higher population densities after 2-day-cultivation than the cells on non-stimulated composites (Khang *et al.,* 2008).

In our earlier studies (Bacakova *et al.*, 2007b; 2008a), carbon nanotubes were used for the creation of composite materials by their mixing with terpolymer of polytetrafluoroethylene, polyvinyldifluoride and polypropylene (PTFE/PVDF/PP) or polysulfone (PSU), i.e., polymers which have been considered to be promising for the construction of bone implants. For example, PTFE/PVDF/PP has been tested as a material for septal nasal reconstruction (Scierski *et al.*, 2007). PSU was used for the creation of composites with bioactive glass particles for potential bone and cartilage tissue engineering (Zhang et al., 2002; Orefice et al., 2007) or for fabrication of bone joint screws (Jan & Grzegorz 2005).

In our experiments, the carbon nanotubes were expected to reinforce the relatively soft and elastic polymeric materials, and thus to improve their mechanical properties for hard tissue surgery. The other desired function of nanotubes was the formation of prominences in nanoscale on the material surface, which could promote its colonization with bone cells.

The PTFE/PVDF/PP-nanotube composites were prepared from a commercially available PTFE/PVDF/PP terpolymer (density of 1600 g/dm^3, Aldrich Chemical Co., U.S.A.) and single-wall carbon nanohorns (SWCNH; belonging to the single-wall nanotube family) or high crystalline electric arc multi-wall nanotubes (MWCNT). Both types of nanoparticles were purchased from NanoCraft Inc., Renton, U.S.A. SWCNH were 2 to 3 nm in diameter, 30 to 50 nm in length, and 19^o closed end (referred to as a horn). The diameter of MWCNT ranged from 5 to 20 nm and the length from 300 to 2000 nm. PTFE/PVDF/PP was dissolved in acetone to a concentration of 0.1 g/ml, and mixed with 2, 4, 6 or 8 wt. % of SWCNH or MWCNT. The suspensions were then exposed to ultrasound in a PARMER INSTRUMENTS sonicator (model CP 130PB, power 130W, frequency 20 kHz) for 10 minutes at 20^o C in order to prevent clustering of the nanoparticles. Finally, the suspensions were poured on to Petri dishes and left to evaporate the solvent (Bacakova *et al.*, 2007b, 2008a).

The addition of SWCNH or MWCNT to the PTFE/PVDF/PP terpolymer markedly improved several parameters of the adhesion and growth of human osteoblast-like MG 63 cells (Bacakova *et al.*, 2007b, 2008a). They were well-spread, polygonal, and contained distinct beta-actin filament bundles, whereas most cells on the pure terpolymer were less spread or even round and clustered into aggregates (Fig. 7). The enzyme-linked immunosorbent assay (ELISA) revealed that the cells on the material with 4 wt. % of SWCNH contained a higher concentration of vinculin (by 64 % and 69 %), a component of focal adhesion plaques, in comparison with the values in cells on the pure terpolymer and tissue culture polystyrene, respectively. The concentration of talin, another important integrin-associated focal adhesion protein, was also higher in cells grown on terpolymer samples with 4 and 8 wt.% of SWCNH (by 35 % and 28 %, respectively). In addition, the cells on carbon nanotube-terpolymer composites were more active in proliferation, which was most apparent on samples with 4 wt. % of MWCNT. On day 7, the cells on this composite reached a population density 4.5 times higher (228 000 ± 10 050 cells/cm^2) than the density on the unmodified PTFE/PVDF/PP (50 300 ± 5 400 cells/cm^2).

After the addition of SWCNH or MWCNT, the wettability of the composite material was relatively low (sessile water drop contact angle from 99 ± 7^o to 105 ± 2^o) and unchanged in comparison with the non-modified terpolymer (contact angle 100 ± 4^o). However, the addition of carbon nanotubes significantly increased the nano- and submicron-scale surface roughness. The R_a parameter (i.e., departures of the roughness profile from the mean line) measured by AFM, ranged from 101 ± 15 nm to 150 ± 23 nm on the nanotube-modified samples, whereas on the pure terpolymer, it was only 30 ± 5 nm. Thus, the increased nano- and submicron-scale surface roughness could explain the beneficial effects of the terpolymer-nanotube composites on the adhesion and growth of MG 63 cells.

On the other hand, the terpolymer-carbon nanotube composites also displayed microscale surface roughness, ranging from 0.59 ± 0.1 μm to 2.22 ± 0.36 μm in the composites with 2 to 8 wt. % of SWCNT, and from 0.41 ± 0.01 μm to 1.63 ± 0.3 μm in the material with 2 to 8 wt. % of MWCNT, as measured by surface profilometry (T500 Hommel Tester, Hommelwerke Co., Germany). The microscale roughness was most probably due to clustering of carbon nanotubes and to prominences of these microclusters on the material surface (Bacakova *et al.,* 2007b, 2008a). An increase in the microscale surface roughness in polymer-carbon nanotube composites has been considered as a factor decreasing the colonization of the composites with cells. For example, on poly(3-hydroxybutyrate)/bioactive glass composites with MWCNT, the cell population density and growth rate of MG 63 cells decreased proportionally to the increasing concentrations of MWCNT (2, 4, 7 wt. %) and increasing microscale surface roughness (RMS from 6 ± 2 to 10 ± 2 μm) of the material (Misra *et al.,* 2010). Also in our study, the cell adhesion and growth of MG 63 cells (evaluated by the concentration of integrin-associated proteins talin and vinculin and the cell population density) was, in most cases, the highest on composites with 4 wt. % of SWCNT or MWCNT (R_a in both cases about 1 μm) and then decreased (Bacakova *et al.,* 2008a).

The polysulfone-nanotube composites were prepared by a similar manner from a commercially available polysulfone (Aldrich Chemical Co., U.S.A.) and SWCNH or MWCNT referred to above. PSU was dissolved in dichloromethane to a concentration of 0.1 g/ml and mixed with 0.5, 1.0 or 2.0 wt.% of SWCNH or MWCNT. The suspensions were then sonicated, poured on to Petri dishes and left to evaporate the solvent (Bacakova *et al.,* 2008a).

The addition on carbon nanotubes to PSU usually did not significantly influence the adhesion, spreading, morphology and growth of MG 63 cells in cultures on these materials (Fig. 7). From days 1 to 5 after seeding, the cell numbers on these composites were usually similar to the values found on the pure PSU. Only the cell adhesion area, measured on day 3 after seeding, was significantly larger on PSU with 2 wt. % of MWCNT (1 770 ± 90 μm^2) than on pristine PSU (1 330 ± 70 μm^2) and cell culture polystyrene dishes (1 400 ± 110 μm^2). These results could be explained by a relatively higher surface hydrophilicity of the pure PSU (water drop contact angle 85 ± 5°) than of the terpolymer PTFE/PVDF/PP (contact angle 100 ± 4°), which might mask the supportive effects of the surface nano-roughness, created by the addition of carbon nanotubes (R_a from 11 ± 4 nm to 27 ± 8 nm *versus* 4 ± 2 nm on the pure PSU, as measured by AFM), on the cell colonization. After the addition of carbon nanotubes, the surface hydrophilicity of the materials slightly decreased on average (i.e., the water drop contact angle increased from 85.0 ± 5° to 93 ± 4°), but these differences were not statistically significant.

Also in the form of thin films, carbon nanotubes acted as good substrates for cell colonization. Carbon nanotubes deposited on various substrates, such as polycarbonate membranes (Aoki *et al.,* 2007), glass coverslips (Holy *et al.,* 2009), titanium (Terada *et al.,* 2009), silicone rubber (Matsuoka *et al.,* 2009), or pressed in compacts (Li *et al.,* 2009a) markedly improved the adhesion, proliferation and differentiation of cells in cultures on these films in comparison with the non-coated materials or pure graphite. Similarly as in the composites of carbon nanotubes with polymers and ceramics, these favorable effects were mediated by an increased adsorption of specific proteins promoting cell adhesion, growth and differentiation, such as cell adhesion-mediating proteins from the serum of the culture medium (Aoki *et al.;* 2007, Li *et al.,* 2009a) and bone morphogenetic protein-2 (Li *et al.,* 2009b), and particularly by the electrical activity of carbon nanotubes (Zanello *et al.,* 2006). The electroactivity of carbon nanotube films makes these materials advantageous for tissue engineering applications involving electrically excitable tissues, such as muscles and nerves.

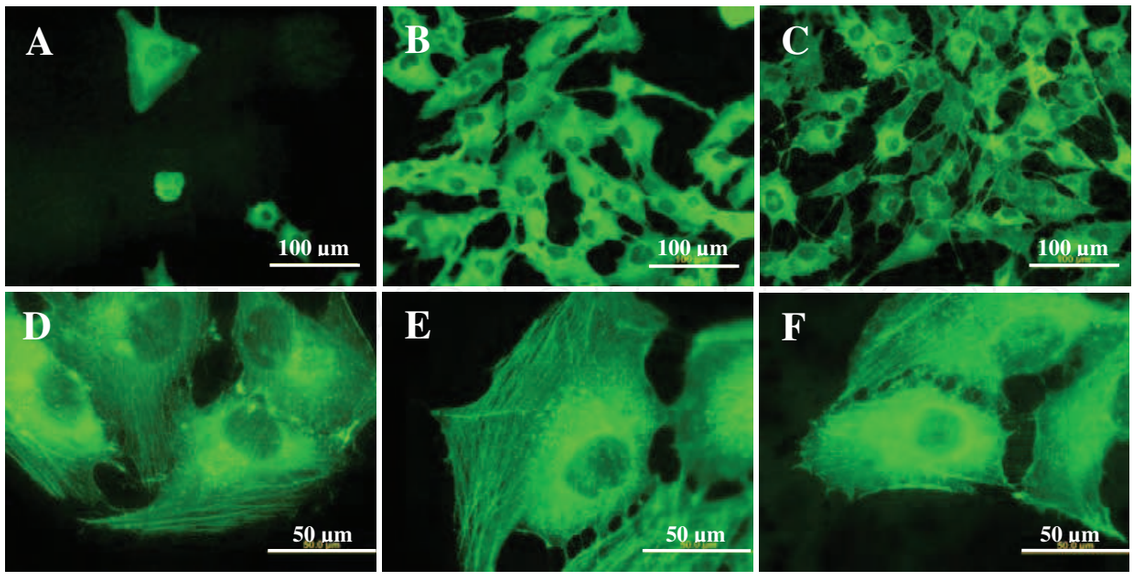

Fig. 7. Immunofluorescence staining of β-actin in human osteoblast-like MG 63 cells on day 3 after seeding on a terpolymer of polytetrafluoroethylene, polyvinyldifluoride and polypropylene (**A**), terpolymer mixed with 4 wt.% of SWCNH (**B**), terpolymer mixed with 4 wt.% of MWCNT (**C**), pure polysulfone (**D**), polysulfone with 2 wt.% of SWCNH (**E**) and polysulfone with 2 wt.% MWCNT (**F**). Olympus IX 51 epifluorescence microscope, DP 70 digital camera. Obj. 20, bar=100 µm (**A-C**), obj. 100x, bar = 20 µm (**D-F**).

For example, SWCNT films sprayed on glass coverslips promoted the outgrowth of neurites and enlargement of the neuron cell body area in hippocampal neurons isolated from newborn rats (Malarkey *et al.*, 2009). The hybrid neuroblastoma*glioma cell line NG108, a model of neuronal cells, and also primary rat peripheral neurons, were electrically coupled to conductive SWCNT films and showed robust voltage-activated currents when electrically stimulated through these substrates (Liopo *et al.*, 2006). Also mouse embryonic neural stem cells, isolated from the brain cortex and seeded on layer-by-layer assembled SWCNT-polyelectrolyte multilayer thin films, were successfully differentiated to neurons, astrocytes, and oligodendrocytes with clear formation of neurites. The neurite outgrowth and expression of specific cell type markers, such as nestin (a marker of neuronal stem cells), microtubule-associated protein 2 (MAP2; a marker of neurons), glial fibrillary acidic protein (anti-GFAP; a marker of astrocytes) and oligodendrocyte marker (O4) in cells cultured on the SWCNT films were similar as on poly-L-ornithine, i.e., one of the most widely used growth substrata for neural stem cells (Jan and Kotov 2007).

Not only continuous films, but also micropatterned carbon nanotube films have been applied for directed adhesion and growth of osteoblasts and neurons. For example, MWCNT were deposited by a hot embossing imprint lithography process on polycarbonate substrates, where they formed 28 different patterns of microscale lanes and circles. The feature diameters and spacing ranged from 9 to 76 µm. Osteoblast-like MC3T3-E1 cells seeded on these surfaces showed a maximum alignment (55 ± 6% of cells) to the microlane patterns with the lane diameter of 16 µm and spacing of 14 µm, and no significant alignment to microcircle patterns (Eliason *et al.*, 2008). Microdomains of carbon nanotubes (CNT) patterned on non-adhesive substrates, such as clean glass or quartz surfaces, also functioned as effective anchoring sites for neurons and glial cells *in vitro*, and thus provided a means to

form complex, engineered, interconnected neuronal networks with pre-designed geometry via utilizing the self-assembly process of neurons. Depositing these CNT islands onto a multielectrode array chip can also facilitate electrical interfacing between the electrodes and the neurons (David-Pur *et al.,* 2010). In addition, the communication between neurites of neurons attached to different nanotube-containing domains induce a mechanical tension in the neuronal network, which serves as a signal for survival of the axonal branch and perhaps for the subsequent formation of synapses (Eliason *et al.,* 2008). Neuronal networks developed on surfaces micropatterned with CNT domains can be utilized not only for neural tissue engineering, but also as advanced neuro-chips for bio-sensing applications, e.g., drug and toxin detection (Sorkin *et al.,* 2006).

Carbon nanotube films can be deposited not only on planar 2D substrates, but also on three-dimensional matrices, i.e., on the walls of pores inside sponge-like collagenous scaffolds for bone tissue engineering. MWCNT deposited on these scaffolds improved the ingrowth of mouse osteoblast MC3T3-E1 cells and human osteosarcoma SaOs-2 cells inside the scaffolds, increased the strength of the cell adhesion and cell number (measured by DNA content), when compared to the scaffolds without nanotubes (Hirata *et al.,* 2009, 2010).

Despite all of these encouraging results, the potential cytotoxicity of carbon nanotubes should also be taken into account. Cytotoxicity of carbon nanotubes were mainly reported in cases when the nanotubes were dispersed in a liquid environment and could penentrate through the cell membrane inside the cells. For example, multi-wall carbon nanotubes (MWCNT) administered intrascrotally behaved as a carcinogen and induced intraperitoneally-disseminated mesothelioma in male Fischer 344 rats (Sakamoto *et al.,* 2009). Carboxylated SWCNT and MWCNT, suspended in the culture medium (concentrations 3, 6 and 30 μg/ml) and added to multipotent mesenchymal stem cells decreased the proliferation, viability, osteogenic differentiation (measured by the activity of alkaline phosphatase), matrix mineralization and also adipogenic differentiation (determined by staining intracytoplasmic lipids with Oil Red O) in these cells. SEM and TEM images revealed that carbon nanotubes might interact with proteins located on the cell membrane or in the cytoplasm, which has a further impact on subsequent cellular signaling pathways. Q-PCR results and Western blot analysis together verified that the inhibition of proliferation and osteogenic differentiation of MSCs may be modulated through a Smad protein-dependent bone morphogenetic protein signaling pathway (Liu *et al.,* 2010).

In addition, carbon nanotubes were revealed to act as cytotoxic not only in suspension, but also in the form of films. Thin films consisting of a SWCNT network, deposited on glass coverslips, were inhibitory to the proliferation, viability, and neuritegenesis of rat pheochromocytoma PC12 cells, and also to the proliferation of human fetal osteoblasts cultured on the top of these substrates, whereas these effects were not observed in cells grown on reduced graphene oxide films. As shown by MTT assay, based on the reduction of a tetrazolium bromide to a purple formazan in living cells, the SWCNT network decreased the activity of mitochondrial enzymes. However, at the same time, similar conductive carbon nanotube networks have been used to electrically stimulate neurons, facilitated propagation of action potentials, boosted neuronal electrical signaling and have been considered to be promising for neural tissue engineering (Agarwal *et al.,* 2010).

8. Conclusion and further perspectives

It can be concluded that all carbon-based materials discussed in this chapter, i.e., hydrocarbon plasma polymers and amorphous carbon (especially when enriched with Ti),

nanocrystalline diamond films (particularly those doped with boron), pyrolytic graphite/carbon, fullerenes C_{60}, binary C_{60}/Ti composites and carbon nanotube-containing substrates provided good supports for the adhesion and growth of cell types present in the bone tissue, such as osteoblasts, endothelial cells or vascular smooth muscle cells. In the form of thin films, all these materials could be used for the coating of bone implants, in which a firm and fast integration with the surrounding bone tissue is desirable, e.g., bone-anchoring parts of joint prostheses or dental replacements. For this purpose, nanocrystalline diamond films are particularly suitable, because they are mechanically and chemically resistant, non-cytotoxic and provide excellent support for the adhesion, spreading, viability, growth and maturation of osteogenic cells. Their beneficial effect on cell colonization can be further enhanced by boron doping, which renders these films electrically conductive and thus enabling electrical stimulation of cells. Electrical conductivity and increased adsorption of molecules mediating cell adhesion or stimulating osteogenic cell differentiation is also characteristic for carbon nanotubes; however, their potential cytotoxicity should be taken into account. Cytotoxicity is also a main risk of fullerene-based films, although in our studies, these films supported the colonization with osteogenic cells to a similar extent as on standard cell culture substrates, such as polystyrene dishes and microscopic glass coverslips. Moreover, binary C_{60}/Ti composite films did not cause DNA damage, as revealed by immunoflurescence of markers of DNA damage response, such as gamma-H2AX and 53BP1. In addition, fullerenes, C_{60}/Ti composites, carbon nanotubes and nanocrystalline diamond can be deposited in the form of micropatterned surfaces for regionally-selective adhesion, directed growth and controlled function of cells. Micropatterned and electroconductive substrates also have great potential to be applied for the construction of biosensors and biostimulators.

9. Acknowledgements

This study was supported by the Academy of Sciences of the Czech Republic (grants No. KAN101120701, KAN400480701, KAN400100701 and IAAX00100902), and the Grant Agency of the Czech Republic (grant No. P108/10/1858). We also wish to thank to Dr. Ken Haenen (Institute for Materials Research, Hasselt University & Division IMOMEC, Belgium) for the growth of boron-doped diamond thin films, Dr. Bohuslav Rezek (Institute of Physics, Acad. Sci. CR) for his characterization of diamond thin films, and Mrs. Jana Vobornikova (Inst. Physiol., Acad. Sci. CR) for her excellent technical assistance in the manuscript preparation. Mrs. Sherryl Ann Vacik (Pangrac & Associates, Angel Fire, New Mexico, U.S.A.) is gratefully acknowledged for her language revision of the manuscript.

10. References

Abbas, A.; Vercaigne-Marko, D.; Supiot, P.; Bocquet, B.; Vivien, C. & Guillochon, D. (2009). Covalent attachment of trypsin on plasma polymerized allylamine. *Colloids Surf B Biointerfaces* 73: 315-324

Agarwal, S.; Zhou, X.; Ye, F.; He, Q.; Chen, G.C.; Soo, J.; Boey, F.; Zhang, H. & Chen, P. (2010). Interfacing live cells with nanocarbon substrates. *Langmuir* 26: 2244-2247

Amaral, M.; Dias, A.G.; Gomes, P.S.; Lopes, M.A.; Silva, R.F.; Santos, J.D. & Fernandes, M.H. (2008). Nanocrystalline diamond: In vitro biocompatibility assessment by MG 63 and human bone marrow cells cultures. *J Biomater Res A* 87: 91-99

Aoki, N.; Akasaka, T.; Watari, F. & Yokoyama, A. (2007). Carbon nanotubes as scaffolds for cell culture and effect on cellular functions. *Dent Mater J* 26: 178-185

Bacakova, L.; Mares, V.; Lisa, V. & Svorcik, V. (2000). Molecular mechanisms of improved adhesion and growth of an endothelial cell line cultured on polystyrene implanted with fluorine ions. *Biomaterials* 21: 1173-1179

Bacakova, L.; Walachova, K.; Svorcik, V. & Hnatowicz, V. (2001a). Adhesion and proliferation of rat vascular smooth muscle cells (VSMC) on polyethylene implanted with O^+ and C^+ ions. *J Biomater Sci Polym Ed* 12: 817-834

Bacakova, L.; Stary, V.; Kofronova, O. & Lisa, V. (2001b). Polishing and coating carbon fiber-reinforced carbon composites with a carbon-titanium layer enhances adhesion and growth of osteoblast-like MG63 cells and vascular smooth muscle cells in vitro. *J Biomed Mater Res* 54: 567-578

Bacakova, L.; Filova, E.; Rypacek, F.; Svorcik, V. & Stary, V. (2004). Cell adhesion on artificial materials for tissue engineering. *Physiol Res* 53 Suppl. 1: S35-S45

Bacakova, L.; Filova, E.; Kubies, D.; Machova, L.; Proks, V.; Malinova, V.; Lisa, V. & Rypacek, F. (2007a). Adhesion and growth of vascular smooth muscle cells in cultures on bioactive RGD peptide-carrying polylactides. *J Mater Sci Mater Med* 18: 1317-1323

Bacakova, L.; Grausova, L.; Vacik, J.; Fraczek, A.; Blazewicz, S.; Kromka, A.; Vanecek, M. & Svorcik, V. (2007b). Improved adhesion and growth of human osteoblast-like MG 63 cells on biomaterials modified with carbon nanoparticles. *Diamond Relat Mater* 16: 2133-2140

Bacakova, L.; Grausova, L.; Vandrovcova, M.; Vacik, J.; Frazcek, A.; Blazewicz, S.; Kromka, A.; Vanecek, M.; Nesladek, M.; Svorcik, V. & Kopecek, M. (2008a). Carbon nanoparticles as substrates for cell adhesion and growth. In: *Nanoparticles: New Research.* Simone Luca Lombardi, (Ed.), pp. 39-107, Nova Science Publishers, Inc., ISBN: 978-1-60456-704-5 Hauppauge, New York

Bacakova, L.; Koshelyev, H.; Noskova, L.; Choukourov, A.; Benada, O.; Mackova, A.; Lisa, V. & Biederman, H. (2008b). Vascular endothelial cells in cultures on nanocomposite silver/hydrocarbon plasma polymer films with antimicrobial activity. *J Optoelectron Adv Mater* 10: 2082-2087

Bacakova, L. & Svorcik, V. (2008). Cell colonization control by physical and chemical modification of materials, In: *Cell Growth Processes: New Research,* Daiki Kimura, (Ed.), pp. 5-56, Nova Science Publishers, Inc., ISBN: 978-1-60456-123-6, Hauppauge, New York

Balani, K.; Anderson, R.; Laha, T.; Andara, M.; Tercero, J.; Crumpler, E. & Agarwal, A. (2007). Plasma-sprayed carbon nanotube reinforced hydroxyapatite coatings and their interaction with human osteoblasts in vitro. *Biomaterials* 28: 618-624

Bekker-Jensen, S.; Lukas, C.; Kitagawa, R.; Melander, F.; Kastan, M.B.; Bartek, J. & Lukas, J. (2006). Spatial organization of the mammalian genome surveillance machinery in response to DNA strand breaks. *J Cell Biol* 173: 195-206

Bernasek, T.L.; Stahl, J.L. & Pupello, D. (2009). Pyrolytic carbon endoprosthetic replacement for osteonecrosis and femoral fracture of the hip: a pilot study. *Clin Orthop Relat Res* 467: 1826-1832

Bettinger, C.J.; Bruggeman, J.P.; Misra, A.; Borenstein, J.T. & Langer, R. (2009). Biocompatibility of biodegradable semiconducting melanin films for nerve tissue engineering. *Biomaterials* 30: 3050-3057

Biederman, H. (2004). *Plasma polymer films.* Biederman, H., (Ed.), Imperial College Press, ISBN: 1-86094-467-1, London

Bondar, V.S.; Pozdnyakova, I.O. & Puzyr, A.P. (2004). Applications of nanodiamonds for separation and purification of proteins. *Phys Solid State* 46: 758-760

Bruinink, A.; Schroeder, A.; Francz, G. & Hauert, R. (2005). In vitro studies on the effect of delaminated a-C:H film fragments on bone marrow cell cultures. *Biomaterials* 26: 3487-3494

Cenni, E.; Granchi, D.; Arciola, C.R.; Ciapetti, G.; Savarino, L.; Stea, S.; Cavedagna, D.; Di Leo, A. & Pizzoferrato, A. (1995). Adhesive protein expression on endothelial cells after contact in vitro with polyethylene terephthalate coated with pyrolytic carbon. *Biomaterials* 16: 1223-1227

Cenni, E.; Granchi, D.; Ciapetti, G.; Savarino, L.; Corradini, A. & Di Leo, A. (2000). Cytokine expression in vitro by cultured human endothelial cells in contact with polyethylene terephthalate coated with pyrolytic carbon and collagen. *J Biomed Mater Res* 50: 483-489

Chai, F.; Mathis, N.; Blanchemain, N.; Meunier, C. & Hildebrand, H.F. (2008) Osteoblast interaction with DLC-coated Si substrates. *Acta Biomater* 4: 1369-1381

Chen, Y.W., Hwang, K.C., Yen, C.C. & Lai, Y.L. (2004). Fullerene derivatives protect against oxidative stress in RAW 264.7 cells and ischemia-reperfused lungs. *Am J Physiol Regul Integr Comp Physiol* 287: R21-R26

Chu, L.Q.: Knoll, W. & Förch, R. (2009). Plasma polymerized non-fouling thin films for DNA immobilization. *Biosens Bioelectron* 25: 519-522

Clem, W.C.; Chowdhury, S.; Catledge, S.A.; Weimer, J.J.; Shaikh, F.M.; Hennessy, K.M.; Konovalov, V.V.; Hill, M.R.; Waterfeld, A.; Bellis, S.L. & Vohra, Y.K. (2008). Mesenchymal stem cell interaction with ultra-smooth nanostructured diamond for wear-resistant orthopaedic implants. *Biomaterials* 29: 3461-3468

Coelho, N.M.; González-García, C.; Planell, J.A.; Salmerón-Sánchez, M. & Altankov, G. (2010). Different assembly of type IV collagen on hydrophilic and hydrophobic substrata alters endothelial cells interaction. *Eur Cell Mater* 19: 262-272

David-Pur, M.; Shein, M. & Hanein, Y. (2010). Carbon nanotube-based neurochips. *Methods Mol Biol* 625: 171-177

Dellinger, A.; Zhou, Z.; Lenk, R.; MacFarland, D. & Kepley, C.L. (2009) Fullerene nanomaterials inhibit phorbol myristate acetate-induced inflammation. *Exp Dermatol* 18: 1079-1081

Deshpande, P.; Notara, M.; Bullett, N.; Daniels, J.T.; Haddow, D.B. & MacNeil, S. (2009). Development of a surface-modified contact lens for the transfer of cultured limbal epithelial cells to the cornea for ocular surface diseases. *Tissue Eng Part A* 15: 2889-2902

Eliason, M.T.; Sunden, E.O.; Cannon, A.H.; Graham, S.; García, A.J. & King, W.P. (2008). Polymer cell culture substrates with micropatterned carbon nanotubes. *J Biomed Mater Res A* 86: 996-1001

Ekstrand, K. & Hirsch, J.M. (2008). Malignant tumors of the maxilla: virtual planning and real-time rehabilitation with custom-made R-zygoma fixtures and carbon-graphite fiber-reinforced polymer prosthesis. *Clin Implant Dent Relat Res* 10: 23-29

Filova, E.; Bullett, N.A.; Bacakova, L.; Grausova, L.; Haycock, J.W.; Hlucilova, J.; Klima, J. & Shard, A. (2009). Regionally-selective cell colonization of micropatterned surfaces prepared by plasma polymerization of acrylic acid and 1,7-octadiene. *Physiol Res* 58: 669-684

Gajewski, W.; Achatz, P.; Williams, O.; Haenen, K.; Bustarret, E.; Stutzmann, M. & Garrido, J. (2009). Electronic and optical properties of boron-doped nanocrystalline diamond films. *Physical Review B* 79: 045206

Gelderman, M.P.; Simakova, O.; Clogston, J.D.; Patri, A.K.; Siddiqui, S.F.; Vostal, A.C. & Simak, J. (2008). Adverse effects of fullerenes on endothelial cells: fullerenol C60(OH)24 induced tissue factor and ICAM-I membrane expression and apoptosis in vitro. *Int J Nanomedicine* 3: 59-68

Goessl, A.; Garrison MD.; Lhoest, JB. & Hoffman, A.S. (2001). Plasma lithography--thin-film patterning of polymeric biomaterials by RF plasma polymerization I: Surface preparation and analysis. *J Biomater Sci Polym Ed* 12: 721-738

Gomez, N. & Schmidt, C.E. (2007). Nerve growth factor-immobilized polypyrrole: bioactive electrically conducting polymer for enhanced neurite extension. *J Biomed Mater Res A* 81: 135-149

Gonzales, K.A.; Wilson, L.J.; Wu, W. & Nancollas, G.H. (2002). Synthesis and in vitro characterization of tissue-selective fullerene: vectoring C60(OH)16AMBP to mineralized bone. *Bioorg Med Chem* 10: 1991-1997

Grausova, L.; Kromka, A.; Bacakova, L.; Potocky, S.; Vanecek, M. & Lisa, V. (2008). Bone and vascular endothelial cells in cultures on nanocrystalline diamond films. *Diamond Relat Mater* 17: 1405–1409

Grausova, L.; Bacakova, L.; Kromka, A.; Vanecek, M. & Lisa, V. (2009a). Molecular markers of adhesion, maturation and immune activation of human osteoblast-like MG 63 cells on nanocrystalline diamond films. *Diamond Relat Mater* 18: 258–263

Grausova, L.; Bacakova, L.; Kromka, A.; Potocky, S.; Vanecek, M.; Nesladek, M. & Lisa, V. (2009b). Nanodiamond as a promising material for bone tissue engineering. *J Nanosci Nanotechnol* 9: 3524-3534

Grausova, L.; Vacik, J.; Vorlicek, V.; Svorcik, V.; Slepicka, P.; Bilkova, P.; Vandrovcova, M.; Lisa, V. & Bacakova, L. (2009c). Fullerene C_{60} films of continuous and micropatterned morphology as substrates for adhesion and growth of bone cells. *Diamond Relat Mater* 18: 578–586

Grausova, L.; Vacik, J.; Bilkova, P.; Vorlicek, V.; Svorcik, V.; Soukup, D.; Bacakova, M.; Lisa, V. & Bacakova, L. (2009d) Regionally-selective adhesion and growth of human osteoblast-like MG 63 cells on micropatterned fullerene C60 layers. *J Optoelectron Adv Mater* 10: 2071-2076

Grinevich, A.; Bacakova, L.; Choukourov, A.; Boldyryeva, H.; Pihosh, Y.; Slavinska, D.; Noskova, L.; Skuciova, M.; Lisa, V. & Biederman, H. (2009). Nanocomposite Ti/hydrocarbon plasma polymer films from reactive magnetron sputtering as growth supports for osteoblast-like and endothelial cells. *J Biomed Mater Res* 88A: 952–966

Guo, S.; Fogarty, D.P.; Nagel, P.M. & Kandel, S.A. (2007). Scanning tunneling microscopy of surface-adsorbed fullerenes: C_{60}, C_{70}, and C_{84}. *Surf Sci* 601: 994-1000

Hahn, B.D.; Lee, J.M.; Park, D.S.; Choi, J.J.; Ryu, J.; Yoon, W.H.; Lee, B.K.; Shin, D.S. & Kim, H.E. (2009). Mechanical and in vitro biological performances of hydroxyapatite-carbon nanotube composite coatings deposited on Ti by aerosol deposition. *Acta Biomater* 5: 3205-3214

He, J.; Zhou, W.; Zhou, X.; Zhong, X.; Zhang, X.; Wan, P.; Zhu, B. & Chen, W. (2008). The anatase phase of nanotopography titania plays an important role on osteoblast cell morphology and proliferation. *J Mater Sci Mater Med* 19: 3465-3472

Hidalgo, E.; Bartolome, R.; Barroso, C.; Moreno, A. & Domínguez, C. (1998). Silver nitrate: antimicrobial activity related to cytotoxicity in cultured human fibroblasts. *Skin Pharmacol Appl Skin Physiol* 11: 140-151

Hirata, E.; Uo, M.; Takita, H.; Akasaka, T.; Watari, F. & Yokoyama, A. (2009). Development of a 3D collagen scaffold coated with multiwalled carbon nanotubes. *J Biomed Mater Res B Appl Biomater* 90: 629-634

Hirata, E.; Uo, M.; Nodasaka, Y.; Takita, H.; Ushijima, N.; Akasaka, T.; Watari, F. & Yokoyama, A. (2010). 3D collagen scaffolds coated with multiwalled carbon nanotubes: initial cell attachment to internal surface. *J Biomed Mater Res B Appl Biomater* 93: 544-550

Ho, C.P. & Yasuda, H. (1988). Ultrathin coating of plasma polymer of methane applied on the surface of silicone contact lenses. *J Biomed Mater Res* 22: 919-937

Holy, J.; Perkins, E. & Yu, X. (2009). Differentiation of pluripotent stem cells on multiwalled carbon nanotubes. *Conf Proc IEEE Eng Med Biol Soc* 2009: 6022-6025

Hornez, J.C.; Chai, F.; Monchau, F.; Blanchemain, N.; Descamps, M. & Hildebrand, H.F. (2007). Biological and physico-chemical assessment of hydroxyapatite (HA) with different porosity. *Biomol Eng* 24: 505-509

Hu, Z.; Liu, S.; Wei, Y.; Tong, E.; Cao, F. & Guan, W. (2007a). Synthesis of glutathione C60 derivative and its protective effect on hydrogen peroxide-induced apoptosis in rat pheochromocytoma cells. *Neurosci Lett* 429: 81-86

Hu, Z.; Guan, W.; Wang, W.; Huang, L.; Xing, H. & Zhu, Z. (2007b). Synthesis of beta-alanine C60 derivative and its protective effect on hydrogen peroxide-induced apoptosis in rat pheochromocytoma cells. *Cell Biol Int* 31: 798-804

Hu, Z.; Guan, W.; Wang, W.; Huang, L.; Xing, H. & Zhu, Z. (2007c). Protective effect of a novel cystine C(60) derivative on hydrogen peroxide-induced apoptosis in rat pheochromocytoma PC12 cells. *Chem Biol Interact* 167: 135-144

Hu, Z.; Guan, W.; Wang, W.; Zhu, Z. & Wang, Y. (2010). Folacin C60 derivative exerts a protective activity against oxidative stress-induced apoptosis in rat pheochromocytoma cells. *Bioorg Med Chem Lett* 20: 4159-4162

Huang, H.; Pierstorff, E.; Osawa, E. & Ho, D. (2008). Protein-mediated assembly of nanodiamond hydrogels into a biocompatible and biofunctional multilayer nanofilm. *ACS Nano* 2: 203-212

Huang, L.; Terakawa, M.; Zhiyentayev, T.; Huang, Y.Y.; Sawayama, Y.; Jahnke, A.; Tegos, G.P.; Wharton, T. & Hamblin, M.R. (2010). Innovative cationic fullerenes as broad-spectrum light-activated antimicrobials. *Nanomedicine* 6: 442-452

Iijima, S. & Ichihashi, T. (1993). Cobalt-catalysed growth of carbon nanotubes with single-atomic-layer walls. *Nature* 363: 603-605

Iijima, S. (2002). Carbon nanotubes: past, present, and future. *Physica B* 323: 1–5

Ismail, F.S.; Rohanizadeh, R.; Atwa, S.; Mason, R.S.; Ruys, A.J.; Martin, P.J. & Bendavid, A. (2007). The influence of surface chemistry and topography on the contact guidance of MG63 osteoblast cells. *J Mater Sci Mater Med* 18: 705-714

Jackson, M.J.; Robinson, G.M.; Ali, N.; Kousar, Y.; Mei, S.; Gracio, J.; Taylor, H. & Ahmed, W. (2006). Surface engineering of artificial heart valve disks using nanostructured thin films deposited by chemical vapour deposition and sol-gel methods. *J Med Eng Technol* 30: 323-329

Jan, C. & Grzegorz, K. (2005). The study of lifetime of polymer and composite bone joint screws under cyclical loads and in vitro conditions. *J Mater Sci Mater Med* 16: 1051-1060

Jan, E. & Kotov, N.A. (2007). Successful differentiation of mouse neural stem cells on layer-by-layer assembled single-walled carbon nanotube composite. *Nano Lett* 7: 1123-1138

Jeong, S.I.; Jun, I.D.; Choi, M.J.; Nho, Y.C.; Lee, Y.M. & Shin, H. (2008). Development of electroactive and elastic nanofibers that contain polyaniline and poly(L-lactide-co-epsilon-caprolactone) for the control of cell adhesion. *Macromol Biosci* 8: 627-637

Johnson-Lyles, D.N.; Peifley, K.; Lockett, S.; Neun, B.W.; Hansen, M.; Clogston, J.; Stern, S.T. & McNeil, S.E. (2010). Fullerenol cytotoxicity in kidney cells is associated with cytoskeleton disruption, autophagic vacuole accumulation, and mitochondrial dysfunction. *Toxicol Appl Pharmacol*, in press

Jun, I.; Jeong, S. & Shin, H. (2009). The stimulation of myoblast differentiation by electrically conductive sub-micron fibers. *Biomaterials* 30: 2038-2047

Kalbacova, M.; Kalbac, M.; Dunsch, L.; Kromka, A.; Vanecek, M.; Rezek, B.; Hempel, U. & Kmoch, S. (2007). The effect of SWCNT and nano-diamond films on human osteoblast cells. *Phys Stat Sol (b)* 244: 4356-4359

Kalbacova, M.; Michalikova, L.; Baresova, V.; Kromka, A.; Rezek, B. & Kmoch, S. (2008). Adhesion of osteoblasts on chemically patterned nanocrystalline diamonds. *Phys Stat Sol (b)* 245: 2124-2127

Kalbacova, M.; Rezek, B.; Baresova, V.; Wolf-Brandstetter, C. & Kromka, A. (2009). Nanoscale topography of nanocrystalline diamonds promotes differentiation of osteoblasts. *Acta Biomater* 5: 3076-3085

Khang, D.; Kim, S.Y.; Liu-Snyder, P.; Palmore, G.T.; Durbin, S.M. & Webster, T.J. (2007). Enhanced fibronectin adsorption on carbon nanotube/poly(carbonate) urethane: independent role of surface nano-roughness and associated surface energy. *Biomaterials* 28: 4756-4768

Khang, D.; Park, G.E. & Webster, T.J. (2008). Enhanced chondrocyte densities on carbon nanotube composites: the combined role of nanosurface roughness and electrical stimulation. *J Biomed Mater Res A* 86: 253-260

Kim, J.; Park, H.; Jung, D. & Kim, S. (2003). Protein immobilization on plasma-polymerized ethylenediamine-coated glass slides. *Anal Biochem* 313: 41-45

Kobayashi, S.; Ohgoe, Y.; Ozeki, K.; Hirakuri, K. & Aoki, H. (2007). Dissolution effect and cytotoxicity of diamond-like carbon coatings on orthodontic archwires. *J Mater Sci Mater Med* 18: 2263-2268

Kong, X.L.; Huang, L.C.L.; Hsu, C.-M.; Chen, W.-H.; Han, C.-C. & Chang, H.-C. (2005). High-affinity capture of proteins by diamond nanoparticles for mass spectrometric analysis. *Anal Chem* 77: 259-265

Kopecek, M.; Bacakova, L.; Vacik, J.; Fendrych, F.; Vorlicek, V.; Kratochvilova, I.; Lisa, V.; Van Hove, E.; Mer, C.; Bergonzo, P. & Nesladek, M. (2008). Improved adhesion, growth and maturation of human bone-derived cells on nanocrystalline diamond films. *Phys Stat Sol (a)* 205: 2146-2153

Kopova, I.; Bacakova, L.; Vacik, J. & Lavrentiev, V. (2010). No evidence for DNA damage by fullerene (C_{60})–transitional metal (Ti) composites developed for potential bone tissue engineering. The 2nd International Conference on Cellular and Molecular Bioengineering (ICCMB2), Book of Abstracts, p. 21, abstract No. C1013, Nanyang Technological University, School of Chemical & Biomedical Engineering, Singapore, August 2 - 4, 2010

Kromka, A.; Rezek, B.; Remes, Z.; Michalka, M.; Ledinsky, M.; Zemek, J.; Potmesil, J. & Vanecek M. (2008). Formation of continuous nanocrystalline diamond layer on glass and silicon at low temperatures. *Chem Vap Deposition* 14: 181-186

Kromka, A.; Grausova, L.; Bacakova, L.; Vacik, J.; Rezek, B.; Vanecek, M.; Williams, O.A. & Haenen, K. (2010). Semiconducting to metallic-like boron doping of nanocrystalline diamond films and its effect on osteoblastic cells. *Diamond Relat Mater* 19: 190-195

Kroto, H.W.; Heath, J.R.; O'Brien, S.C.; Curl, R.F. & Smalley, R.E. (1985). C_{60}: Buckminsterfullerene. *Nature* 318: 162-163

Kwok, S.C.; Yang, P.; Wang, J.; Liu, X. & Chu, P.K. (2004). Hemocompatibility of nitrogen-doped, hydrogen-free diamond-like carbon prepared by nitrogen plasma immersion ion implantation-deposition. *J Biomed Mater Res A* 70: 107-114

Lahiri, D.; Rouzaud, F.; Namin, S.; Keshri, A.K.; Valdes, J.J.; Kos, L.; Tsoukias, N.; & Agarwal, A. (2009). Carbon nanotube reinforced polylactide-caprolactone copolymer: mechanical strengthening and interaction with human osteoblasts in vitro. *ACS Appl Mater Interfaces* 1: 2470-2476

Lao, F.; Chen, L.; Li, W.; Ge, C.; Qu, Y.; Sun, Q.; Zhao, Y.; Han, D. & Chen, C. (2009). Fullerene nanoparticles selectively enter oxidation-damaged cerebral microvessel endothelial cells and inhibit JNK-related apoptosis. *ACS Nano* 3: 3358-3368

Levi, N.; Hantgan, R.R.; Lively, M.O.; Carroll, D.L. & Prasad, G.L. (2006). C_{60}-fullerenes: detection of intracellular photoluminescence and lack of cytotoxic effects. *J Nanobiotechnol* 4:14

Li, X.; Gao, H.; Uo, M.; Sato, Y.; Akasaka, T.; Feng, Q.; Cui, F.; Liu, X. & Watari, F. (2009a). Effect of carbon nanotubes on cellular functions in vitro. *J Biomed Mater Res A* 91: 132-139

Li, X.; Gao, H.; Uo, M.; Sato, Y.; Akasaka, T.; Abe, S.; Feng, Q.; Cui, F. & Watari, F. (2009b). Maturation of osteoblast-like SaoS2 induced by carbon nanotubes. *Biomed Mater* 4: 015005

Lin, J.; Park, I.W.; Mishra, B.; Pinkas, M.; Moore, J.J.; Anton, J.M.; Kim, K.H.; Voevodin, A.A. & Levashov, E.A. (2009). Processing, structure, and properties of nanostructured multifunctional tribological coatings. *J Nanosci Nanotechnol* 9: 4073-4084

Liopo, A.V.; Stewart, M.P.; Hudson, J.; Tour, J.M. & Pappas, T.C. (2006). Biocompatibility of native and functionalized single-walled carbon nanotubes for neuronal interface. *J Nanosci Nanotechnol* 6: 1365-1374

Liu, D.; Yi, C.; Zhang, D.; Zhang, J. & Yang, M. (2010). Inhibition of proliferation and differentiation of mesenchymal stem cells by carboxylated carbon nanotubes. *ACS Nano* 4: 2185-2195

Liu, J. & Tabata, Y. (2010). Photodynamic therapy of fullerene modified with pullulan on hepatoma cells. *J Drug Target* 18: 602-610

Maeda, R.; Noiri, E.; Isobe, H.; Homma, T.; Tanaka, T.; Negishi, K.; Doi, K.; Fujita, T. & Nakamura, E. (2008). A water-soluble fullerene vesicle alleviates angiotensin II-induced oxidative stress in human umbilical venous endothelial cells. *Hypertens Res* 31: 141-151

Majani, R.; Zelzer, M.; Gadegaard, N.; Rose, F.R. & Alexander, M.R. (2010). Preparation of Caco-2 cell sheets using plasma polymerised acrylic acid as a weak boundary layer. *Biomaterials* 31: 6764-6771

Majid, E.; Male, K.B. & Luong, J.H. (2008). Boron doped diamond biosensor for detection of Escherichia coli. *J Agric Food Chem* 56: 7691-7695

Malarkey, E.B.; Fisher, K.A.; Bekyarova, E.; Liu, W.; Haddon, R.C. & Parpura, V. (2009). Conductive single-walled carbon nanotube substrates modulate neuronal growth. *Nano Lett* 9: 264-268

Marchesan, S.; Da Ros, T.; Spalluto, G.; Balzarini, J. & Prato M. (2005). Anti-HIV properties of cationic fullerene derivatives. *Bioorg Med Chem Lett* 15: 3615-3618

Marcon, L.; Spriet, C.; Coffinier, Y.; Galopin, E.; Rosnoblet, C.; Szunerits, S.; Heliot, L.; Angrand, P.O. & Boukherroub, R. (2010). Cell Adhesion properties on chemically micropatterned boron-doped diamond surfaces. *Langmuir*, in press

Maropis, P.S.; Molinari, J.A.; Appel, B.N. & Baumhammers, A. (1977). Comparative study of vitreous carbon, pyrolytic carbon, pyrolytic graphite/silicon-carbide, and titanium implants in rabbit mandibles. *Oral Surg Oral Med Oral Pathol* 43: 506-512

Matsuoka, M.; Akasaka, T.; Hashimoto, T.; Totsuka, Y. & Watari, F. (2009). Improvement in cell proliferation on silicone rubber by carbon nanotube coating. *Biomed Mater Eng* 19: 155-162

Menzies, D.J.; Cowie, B.; Fong, C.; Forsythe, J.S.; Gengenbach, T.R.; McLean, K.Mm; Puskar, L.; Textor, M.; Thomsen, L.; Tobin, M. & Muir, B.W. (2010). One-step method for generating PEG-like plasma polymer gradients: chemical characterization and analysis of protein interactions. *Langmuir*, in press

Misra, S.K.; Ohashi, F.; Valappil, S.P.; Knowles, J.C.; Roy, I.; Silva, S.R.; Salih, V. & Boccaccini, A.R. (2010). Characterization of carbon nanotube (MWCNT) containing P(3HB)/bioactive glass composites for tissue engineering applications. *Acta Biomater* 6: 735-742

Monties, J.R.; Havlik, P.; Mesana, T.; Trinkl, J.; Tourres, J.L. & Demunck, J.L. (1994). Development of the Marseilles pulsatile rotary blood pump for permanent implantable left ventricular assistance. *Artif Organs* 18: 506-511

Nebel, C.E.; Shin, D.; Rezek, B.; Tokuda, N.; Uetsuka, H. & Watanabe, H. (2007). Diamond and biology. *J R Soc Interface* 4: 439-461

Orefice, R.; Clark, A.; West, J.; Brennan, A. & Hench, L. (2007). Processing, properties, and in vitro bioactivity of polysulfone-bioactive glass composites. *J Biomed Mater Res A* 80: 565-580

Papo, M.J.; Catledge, S.A.; Vohra, Y.K. & Machado, C. (2004). Mechanical wear behavior of nanocrystalline and multilayer diamond coatings on temporomandibular joint implants. *J Mater Sci: Mater Med* 15: 773-777

Pelto, J.; Haimi, S.; Puukilainen, E.; Whitten, P.G.; Spinks, G.M.; Bahrami-Samani, M.; Ritala, M. & Vuorinen, T. (2010). Electroactivity and biocompatibility of polypyrrole-hyaluronic acid multi-walled carbon nanotube composite. *J Biomed Mater Res A* 93: 1056-1067

Pesakova, V.; Klezl, Z.; Balik, K. & Adam, M. (2000). Biomechanical and biological properties of the implant material carbon-carbon composite covered with pyrolytic carbon. *J Mater Sci Mater Med* 11: 793-798

Price, R.L.; Ellison, K.; Haberstroh, K.M. & Webster, T.J. (2004). Nanometer surface roughness increases select osteoblast adhesion on carbon nanofiber compacts. *J Biomed Mater Res A* 70: 129-138

Prylutska, S.V.; Grynyuk, I.I.; Palyvoda, K.O. & Matyshevska, O.P. (2010). Photoinduced cytotoxic effect of fullerenes C60 on transformed T-lymphocytes. *Exp Oncol* 32: 29-32

Rakngarm, A.; Miyashita, Y. & Mutoh, Y. (2008). Formation of hydroxyapatite layer on bioactive Ti and Ti-6Al-4V by simple chemical technique. *J Mater Sci Mater Med* 19: 1953-1961

Rezek, B.; Shin, D. & Nebel, C.E. (2007). Properties of hybridized DNA arrays on single-crystalline undoped and boron-doped (100) diamonds studied by atomic force microscopy in electrolytes. *Langmuir* 23: 7626-7633

Rezek, B.; Michalikova, L.E.; Ukraintsev, E.; Kromka, A. & Kalbacova, M. (2009). Micro-pattern guided adhesion of osteoblasts on diamond surfaces. *Sensors* 9: 3549-3562

Roy, R.K. & Lee, K.R. (2007). Biomedical applications of diamond-like carbon coatings: a review. *J Biomed Mater Res B Appl Biomater* 83: 72-84

Ruiz, A.; Buzanska, L.; Gilliland, D.; Rauscher, H.; Sirghi, L.; Sobanski, T.; Zychowicz, M.; Ceriotti, L.; Bretagnol, F.; Coecke, S.; Colpo, P. & Rossi, F. (2008). Micro-stamped surfaces for the patterned growth of neural stem cells. *Biomaterials* 29: 4766-4774

Rupprecht, S.; Bloch, A.; Rosiwal, S.; Neukam, F.W. & Wiltfang, J. (2002). Examination of the bone-metal interface of titanium implants coated by the microwave plasma chemical vapor deposition method. *Int J Oral Maxillofac Implants* 17: 778-785

Sakamoto, Y.; Nakae, D.; Fukumori, N.; Tayama, K.; Maekawa, A.; Imai, K.; Hirose, A.; Nishimura, T.; Ohashi, N. & Ogata, A. (2009). Induction of mesothelioma by a single intrascrotal administration of multi-wall carbon nanotube in intact male Fischer 344 rats. *J Toxicol Sci* 34: 65-76

Santavirta, S. (2003). Compatibility of the totally replaced hip. Reduction of wear by amorphous diamond coating. *Acta Orthop Scand* Suppl 74: 1-19

Sato, H.; Tsuji, H.; Ikeda, S.; Ikemoto, N.; Ishikawa, J. & Nishimoto, S. (1999). Enhanced growth of human vascular endothelial cells on negative ion (Ag-)-implanted hydrophobic surfaces. *J Biomed Mater Res* 44: 22-30

Sawase, T.; Jimbo, R.; Baba, K.; Shibata, Y.; Ikeda, T. & Atsuta, M. (2008). Photo-induced hydrophilicity enhances initial cell behavior and early bone apposition. *Clin Oral Implants Res* 19: 491-496

Schmidt, C.E.; Shastri, V.R.; Vacanti, J.P. & Langer, R. (1997). Stimulation of neurite outgrowth using an electrically conducting polymer. *Proc Natl Acad Sci U S A* 94: 8948-8953

Schrand, A.M.; Huang, H.; Carlson, C.; Schlager, J.J.; Osawa, E.; Hussain, S.M. & Dai, L. (2007). Are diamond nanoparticles cytotoxic? *J Phys Chem* 111: 2-7

Schroeder, A.; Francz, G.; Bruinink, A.; Hauert, R.; Mayer, J. & Wintermantel, E. (2000). Titanium containing amorphous hydrogenated carbon films (a-C: H/Ti): surface analysis and evaluation of cellular reactions using bone marrow cell cultures in vitro. *Biomaterials* 21: 449-456

Schultz, L.B.; Chehab, N.H.; Malikzay, A. & Halazonetis, T.D. (2000). p53 binding protein 1 (53BP1) is an early participant in the cellular response to DNA double-strand breaks. *J Cell Biol* 151: 1381-1390

Scierski, W.; Polok, A.; Namyslowski, G.; Błazewicz, M.; Pamula, E.; Stodolak, E.; Nozynski, J.; Zwirska-Korczala, K.; Szwarc, K.; Misiolek, M.; Czecior, E.; Turecka, L.; Lisowska, G. & Orecka, B. (2007). Study of selected biomaterials for reconstruction of septal nasal perforation. *Otolaryngol Pol* 61: 842-846

Seyama, M.; Sugimoto, I. & Nakamura, M. (2004). Aroma sensing and indoor air monitoring by quartz crystal resonators with sensory films prepared by sputtering of biomaterials and sintered polymers. *Biosens Bioelectron* 20: 814-824

Shi, X.; Hudson, J.L.; Spicer, P.P.; Tour, J.M.; Krishnamoorti, R. & Mikos, A.G. (2006). Injectable nanocomposites of single-walled carbon nanotubes and biodegradable polymers for bone tissue engineering. *Biomacromolecules* 7: 2237-2242

Shi, G.; Rouabhia, M.; Meng, S. & Zhang, Z. (2008). Electrical stimulation enhances viability of human cutaneous fibroblasts on conductive biodegradable substrates. *J Biomed Mater Res A* 84: 1026-1037

Shtansky, D.V.; Gloushankova, N.A.; Sheveiko, A.N.; Kharitonova, M.A.; Moizhess, T.G.; Levashov, E.A. & Rossi, F. (2005). Design, characterization and testing of Ti-based multicomponent coatings for load-bearing medical applications. *Biomaterials* 26: 2909-2924

Sorkin, R.; Gabay, T.; Blinder, P.; Baranes, D.; Ben-Jacob, E. & Hanein, Y. (2006). Compact self-wiring in cultured neural networks. *J Neural Eng* 3: 95-101

Stary, V.; Bacakova, L.; Hornik, J. & Chmelik, V. (2002). Bio-compatibility of the surface layer of pyrolytic graphite. *Thin Solid Films* 433: 191-198

Stary, V.; Glogar, P.; Bacakova, L.; Hnilica, F.; Chmelik, V.; Korinek, Z.; Gregor, J.; Mares, V. & Lisa, V. (2003). A study of surface properties of composite materials and their influence on the biocompatibility. *Acta Montana* AB 11: 19-36

Straface, E.; Natalini, B.; Monti, D.; Franceschi, C.; Schettini, G.; Bisaglia, M.; Fumelli, C.; Pincelli, C.; Pellicciari, R. & Malorni, W. (1999). C3-fullero-tris-methanodicarboxylic acid protects epithelial cells from radiation-induced anoikia by influencing cell adhesion ability. *FEBS Lett* 454: 335-340

Sun, T.; Jackson, S.; Haycock, J.W. & MacNeil, S. (2006). Culture of skin cells in 3D rather than 2D improves their ability to survive exposure to cytotoxic agents. *J Biotechnol* 122: 372-381

Supronowicz, P.R.; Ajayan, P.M.; Ullmann, K.R.; Arulanandam, B.P.; Metzger, D.W. & Bizios, R. (2002). Novel current-conducting composite substrates for exposing osteoblasts to alternating current stimulation. *J Biomed Mater Res* 59: 499-506

Suzuki, Y.; Yoshimaru, T.; Yamashita, K.; Matsui, T.; Yamaki, M. & Shimizu, K. (2001). Exposure of RBL-2H3 mast cells to Ag(+) induces cell degranulation and mediator release. *Biochem Biophys Res Commun* 283: 707-714

Teixeira, V.; Soares, P.; Martins, A.J.; Carneiro, J. & Cerqueira, F. (2009). Nanocomposite metal amorphous-carbon thin films deposited by hybrid PVD and PECVD technique. *J Nanosci Nanotechnol* 9: 4061-4066

Terada, M.; Abe, S.; Akasaka, T.; Uo, M.; Kitagawa, Y. & Watari, F. (2009). Multiwalled carbon nanotube coating on titanium. *Biomed Mater Eng* 19: 45-52

Thalhammer, A.; Edgington, R.J.; Cingolani, L.A.; Schoepfer, R. & Jackman, R.B. (2010). The use of nanodiamond monolayer coatings to promote the formation of functional neuronal networks. *Biomaterials* 31: 2097-2104

Thierry, B.; Jasieniak, M.; de Smet, L.C.; Vasilev, K. & Griesser, H.J. (2008). Reactive epoxy-functionalized thin films by a pulsed plasma polymerization process. *Langmuir* 24: 10187-10195

Toworfe, G.K.; Composto, R.J.; Shapiro, I.M. & Ducheyne, P. (2006). Nucleation and growth of calcium phosphate on amine-, carboxyl- and hydroxyl-silane self-assembled monolayers. *Biomaterials* 27: 631-642

Tran, H.S.; Puc, M.M.; Hewitt, C.W.; Soll, D.B.; Marra, S.W.; Simonetti, V.A.; Cilley, J.H. & DelRossi, A.J. (1999). Diamond-like carbon coating and plasma or glow discharge treatment of mechanical heart valves. *J Invest Surg* 12: 133-140

Tsai, S.W.; Loughran, M.; Hiratsuka, A.; Yano, K. & Karube, I. (2003). Application of plasma-polymerized films for isoelectric focusing of proteins in a capillary electrophoresis chip. *Analyst* 128: 237-244

Tykhomyrov, A.A.; Nedzvetsky, V.S.; Klochkov, V.K. & Andrievsky, G.V. (2008). Nanostructures of hydrated C60 fullerene (C60HyFn) protect rat brain against alcohol impact and attenuate behavioral impairments of alcoholized animals. *Toxicology* 246: 158-165

Vacik, J.; Lavrentiev, V.; Novotna, K.; Bacakova, L.; Lisa, V.; Vorlicek, V. & Fajgar, R. (2010). Fullerene (C60)–transitional metal (Ti) composites: Structural and biological properties of the thin films. *Diamond Relat Mater* 19: 242-246

Vandrovcova, M.; Vacik, J.; Svorcik, V.; Slepicka, P.; Kasalkova, N.; Vorlicek, V.; Lavrentiev, V.; Vosecek, V.; Grausova, L.; Lisa, V. & Bacakova, L. (2008). Fullerene C60 and hybrid C60/Ti films as substrates for adhesion and growth of bone cells. *Phys Stat Sol (a)* 205: 2252-2261

Vasilev, K.; Sah, V.; Anselme, K,; Ndi, C,; Mateescu, M,; Dollmann, B.; Martinek, P.; Ys, H.; Ploux, L. & Griesser, H.J. (2010). Tunable antibacterial coatings that support mammalian cell growth. *Nano Lett* 10: 202-207

Watari, F.; Takashi, N.; Yokoyama, A.; Uo, M.; Akasaka, T.; Sato, Y.; Abe, S.; Totsuka, Y. & Tohji, K. (2009). Material nanosizing effect on living organisms: non-specific, biointeractive, physical size effects. *J R Soc Interface* 6 Suppl 3: S371-388

Webster, T.J.; Ergun, C.; Doremus, R.H.; Siegel, R.W. & Bizios, R. (2000). Specific proteins mediate enhanced osteoblast adhesion on nanophase ceramics. *J Biomed Mater Res* 51: 475-483

Xu, A.; Chai, Y.; Nohmi, T. & Hei, T.K. (2009). Genotoxic responses to titanium dioxide nanoparticles and fullerene in gpt delta transgenic MEF cells. *Part Fibre Toxicol* 6: 3

Yakobson, B. & Smalley, R.E. (1997). Fullerene nanotubes: C[sub1,000,000) and beyond. *Am Sci* 85, 324-333

Yamawaki, H. & Iwai, N. (2006). Cytotoxicity of water-soluble fullerene in vascular endothelial cells. *Am J Physiol Cell Physiol* 290: C1495-C1502

Yang, L.; Sheldon, B.W. & Webster, T.J. (2009). Orthopedic nano diamond coatings: control of surface properties and their impact on osteoblast adhesion and proliferation. *J Biomed Mater Res A* 91: 548-556

Yang, Z.; Wang, J.; Luo, R.; Maitz, M.F.; Jing, F.; Sun, H. & Huang, N. (2010). The covalent immobilization of heparin to pulsed-plasma polymeric allylamine films on 316L stainless steel and the resulting effects on hemocompatibility. *Biomaterials* 31: 2072-2083

Yildiz, H.; Ha, S.K. & Chang, F.K. (1998a). Composite hip prosthesis design. I. Analysis. *J Biomed Mater Res* 39: 92-101

Yildiz, H.; Chang, F.K. & Goodman, S. (1998b) Composite hip prosthesis design. II. Simulation. *J Biomed Mater Res* 39: 102-119

Zanello, L.P.; Zhao, B.; Hu, H. & Haddon, R.C. (2006). Bone cell proliferation on carbon nanotubes. *Nano Lett* 6: 562-567

Zhang, K.; Ma, Y. & Francis, L.F. (2002). Porous polymer/bioactive glass composites for soft-to-hard tissue interfaces. *J Biomed Mater Res* 61: 551-563

Zhang, Z.H. & Feng, C.L. (2007). The investigation of protein adsorption behaviors on different functionalized polymers films. *Biotechnol J* 2: 743-751

Zhao, J.; Wu, L. & Zhi, J. (2009). Non-enzymatic glucose detection using as-prepared boron-doped diamond thin-film electrodes. *Analyst* 134: 794-799

Zheng, Y.; Liu, D.; Liu, X. & Li, L. (2008). Ti-TiC-TiC/DLC gradient nano-composite film on a biomedical NiTi alloy. *Biomed Mater* 3: 044103

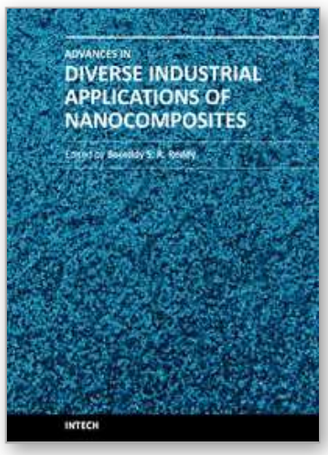

Advances in Diverse Industrial Applications of Nanocomposites
Edited by Dr. Boreddy Reddy

ISBN 978-953-307-202-9
Hard cover, 550 pages
Publisher InTech
Published online 22, March, 2011
Published in print edition March, 2011

Nanocomposites are attractive to researchers both from practical and theoretical point of view because of combination of special properties. Many efforts have been made in the last two decades using novel nanotechnology and nanoscience knowledge in order to get nanomaterials with determined functionality. This book focuses on polymer nanocomposites and their possible divergent applications. There has been enormous interest in the commercialization of nanocomposites for a variety of applications, and a number of these applications can already be found in industry. This book comprehensively deals with the divergent applications of nanocomposites comprising of 22 chapters.

How to reference
In order to correctly reference this scholarly work, feel free to copy and paste the following:

Lucie Bacakova, Lubica Grausova, Jiri Vacik, Alexander Kromka, Hynek Biederman, Andrei Choukourov and Vladimir Stary (2011). Nanocomposite and Nanostructured Carbon-based Films as Growth Substrates for Bone Cells, Advances in Diverse Industrial Applications of Nanocomposites, Dr. Boreddy Reddy (Ed.), ISBN: 978-953-307-202-9, InTech, Available from: http://www.intechopen.com/books/advances-in-diverse-industrial-applications-of-nanocomposites/nanocomposite-and-nanostructured-carbon-based-films-as-growth-substrates-for-bone-cells

INTECH
open science | open minds

InTech Europe
University Campus STeP Ri
Slavka Krautzeka 83/A
51000 Rijeka, Croatia
Phone: +385 (51) 770 447
Fax: +385 (51) 686 166
www.intechopen.com

InTech China
Unit 405, Office Block, Hotel Equatorial Shanghai
No.65, Yan An Road (West), Shanghai, 200040, China
中国上海市延安西路65号上海国际贵都大饭店办公楼405单元
Phone: +86-21-62489820
Fax: +86-21-62489821

IntechOpen